École polytechnique de Louvain

Enhancing the Safety of Firefighters in Intervention with a Wearable Heart Rate Sensor

Author: **Martin BRANS**
Supervisor: **David BOL**
Readers: **Sylvain FAVRESSE, Marco GONZALEZ GONZALEZ, Bertrand LORENT, Laurent FRANCIS**
Academic year 2024–2025
Master [120] in Electro-mechanical Engineering

Acknowledgements

I would like to thank my supervising team for their support, their advice, and their enthusiasm towards my project, and for the courses they worked on and that I had the chance to follow: my supervisor, Professor David Bol, my contact with the Walloon Brabant fire department, Captain Bertrand Lorent, and my assistants, Sylvain Favresse and Marco Gonzalez Gonzalez. I wish Marco a lot of courage for the last few weeks of writing his Ph.D. thesis and I congratulate him in advance for that wonderful achievement.

I would then like to congratulate my brother, Victor, and my sister-in-law, Andréa, for their union that was celebrated in the grandest of fashions. It was an honour to be their witness, and it will always be a pleasure to witness their dedicated love. I wish them happiness above all, and that it may last forever. I would like to wholeheartedly thank them, along with the rest of my family for their unconditional support: Môman, Papou, Laurent, Marie, Tonton, Jamila, Nainaine, Papy, François, Pierre, Arsène and Norah.

I wish also to thank my friends for keeping joy into my world at all times. They all mean so much to me, no matter how far from me they are: the banana lovers, the gnome hunters, the motocross enjoyers, the robot-athlete makers, the robot-superstar makers, the math streamer, the mangakas of the mountains, the Pantera enthusiasts, and all the others. A special thanks to Martin Debowski for simply being the chillest and most brilliant of all guys I've ever known, I still don't know how you endured my endless ramblings in my many times of great difficulty without telling me to go suck an egg.

As this marks the probable end of my studies at EPL, I would like to thank the whole community of the EPL discord for the many great moments I've spent among them, sharing knowledge, memes, music and political stances. As the host of the EPL Drive since 2022, I would like to thank the contributors and administrators, past, present and future, for making this place one of the greatest student platforms for knowledge and assistance.

Abstract

Firefighting is a stressful and physically demanding job, and it can have fatal consequences on the firefighter if the stress (psychological and/or physiological) is not well managed. A review of modern firefighting personal protective equipment shows that electronics already helps in many tactical and safety aspects: it improves communication, perception and coordination. However, vital signs are generally not monitored by these systems. Heart rate, respiration, hydration, body temperature and body movements are all variables that can be monitored to assess the firefighter's level of exhaustion, evaluate their fitness or detect injuries and cardiovascular diseases. For each variable, many sensing techniques tried in the scientific literature are reviewed in this work, although some are not fit for the application. A special focus on heart rate was chosen because it's highly correlated with stress and easy to sense. Photoplethysmography (PPG) was chosen to sense the heart rate because it's simple, cheap and non invasive. A study on the accuracy of open-source heart-rate-tracking algorithms based on PPG is then conducted using two datasets of recorded signals and reference heart rate data. Open-source algorithms perform well in the absence of noise caused by motion, but do not perform sufficiently well when this noise is too dominant. An approach that uses accelerometer data was tested and yielded better results, although not sufficient. More advanced signal processing techniques are therefore required. Finally, a proof-of-concept prototype was successfully built using a PPG sensor evaluation kit. The software was modified to be more robust, although some improvements are to be made. Other aspects, such as power consumption, battery technology and integration into firefighting equipment, also have to be addressed.

Contents

Introduction

Firefighting is a risky and physically demanding job that inherently places firefighters in unpredictable and dangerous environments. Studies have shown that such scenarios cause significant physiological, physical and psychological stress, which can impair both the physical and cognitive performance of the firefighter on duty [1], [2], [3]. Moreover, firefighters tend to be unaware of the levels of stress they experience during their work [2]. The frequency of these high-stress and high-exertion periods make them the leading cause of injury or death in this profession in the USA: 54% of fatalities (29 fatalities) among firefighters in 2019 in the USA were due to overexertion, stress and medical issues, a majority of which were related to heart conditions [4]. Cardiac problems, especially coronary heart disease, tend to be a recurring problem in firefighting [5] because they are caused in the long term by shift work, exposure to smoke, noise, psychological stress, physical workload, heat and dehydration, among other causes [6]. However, a slow decline of the number of yearly fatalities in American firefighters, along with a stable increase of their workforce, indicates that the problem is being resolved [4], [7]. This is in part because the issue has been known for a while, thus professionals and voluntaries alike now have to pass medical checks before being hired and regularly follow specialised fitness programs, along with other measures to improve overall safety [4].

In Belgium, firefighter injuries and deaths are much less numerous, mainly because of the smaller number of habitants in the country. On May 30th 2025, 40-year-old Belgian firefighter Maxime Coessens died doing a reconnaissance task when intervening on a fire at the prison in Lantin. According to local news, he and his team were trapped by a locked door in a confined room where the temperature rose and caused them severe burns. This is known as an “oven effect”. The three other members of the reconnaissance team were hospitalised, but thankfully survived the accident [8]. In 2022, it was the death of 49-year-old Jean-François Spelmans that shocked the community of Belgian firefighters [9]. The sergeant-major died from his wounds after a fire at a construction site in Brussels made an escalator collapse on him [10]. These were the only firefighter fatalities on duty in Belgium since over a decade [11]. According to internal statistics of the Walloon Brabant Fire Department, Belgium counts 27 firefighter deaths during service (i.e., during standby or during an intervention) over the last 30 years, with the latest one being caused by a heart attack in 2025. Interventions also tend

(a) PSS® AirBoss Agile, to be worn by the firefighter.

(b) FireGround, to be operated by the team supervisor.

Figure 1: Example of modern equipment with connectivity from Dräger [12].

to be less likely to cause non lethal injuries: between 2020 and 2022, Belgium counted only 2 injuries for every 1000 fires, compared to 45 in the USA during the same period [11].

Studying and monitoring the stress experienced by firefighters during interventions can be useful to make recommendations regarding fitness standards and mandatory medical evaluations [1]. In addition, this information on the firefighter's condition can aid in the team's decision-making during the intervention. Valuable information for decision-making can also be gathered about the environment or the equipment in real time, which motivates the need for multi-sensor systems [13]. Modern firefighting equipment is already able to sense some information on the wearer's surroundings, well-being and equipment condition, relay it to the firefighter, and even communicate it wirelessly over long ranges to a supervisor. For example, the combination of Dräger's FireGround and PSS® AirBoss, shown in Figure 1, makes it possible to remotely monitor the air reserves of the self-contained breathing apparatus (SCBA) of each individual. Supervisors can then plan in advance when to recall a firefighter with depleting air reserves. In addition, an emergency situation can be signalled by the press of a button on the PSS® AirBoss, or detected via the absence of movement for some time [12]. However, this latter feature tends to be used when the situation is already critical, when the firefighter is in great danger. In the past, some firefighters have lost their lives due to the rest of the team being made aware of the situation too late [14]. Some vital signs such as the heart rate, breathing rate and others are relatively simple to sense and are correlated to the firefighter's level of stress [1]. Therefore, some of these situations can be managed earlier during the intervention by monitoring these vital signs, so that the worst consequences can be avoided. This has yet to be implemented into the existing firefighting systems, which is the purpose of this work. Some attempts have already been made in academia, such as the VitalJacket® of Rodrigues *et al.* [2], or the prototype of Nascimento *et al.* [15]. In fact, the field of wearable health/fitness sensors (for outdoor activities or continuous health monitoring) has already resolved many aspects of sensing vital signs during physical activities. However, some practical aspects regarding the specific case of firefighting have to be addressed, e.g., the reliability of the results, the robustness of the wireless connection, the ergonomics, etc.

For this master's thesis, I collaborated with Captain Bertrand Lorent of the Walloon Brabant Fire Department and with the personnel at UCLouvain to prototype a wearable sensor system that could be integrated into a firefighter's personal protective equipment (PPE) and used during an intervention. Worn on the wrist, this device derives the firefighter's heart rate using photoplethysmography (PPG). It is then able to communicate this result wirelessly to another device using a Bluetooth® Low Energy connection.

The aim of this device is to be a proof of concept, i.e. to serve as a starting point for future development of a system capable of sensing several vital signals during a firefighter's intervention, extract valuable information from them, and communicate its results to already existing equipment with longer-range communication capabilities. It offers an opportunity to tackle some of the challenges proposed by this particular application.

First, Chapter 1 gives an overview of the firefighting PPE, and of the modern variants that provide monitoring and connectivity. From this, the variables that can be monitored in the scope of a master's thesis such as this one are identified and assessed in terms of relevance and practical feasibility, with the help of scientific data and the experience of Captain Lorent.

Next, focusing on heart rate, the principle of PPG is explained in Chapter 2. Different signal processing algorithms are also shown in detail, with which heart rate can be estimated using the extracted PPG signal. These algorithms originate from both scientific literature and open-source software. Their accuracy is evaluated and compared thanks to open-access datasets of PPG sample recordings paired with their ground-truth heart rate value.

Finally, the designed wearable heart rate sensor prototype is presented and characterised in Chapter 3. The choices made when selecting its hardware are explained. The behaviour of the software and the signal processing is also detailed. The prototype is then tested in terms of functionality. Suggested improvements are given throughout the chapter.

This work has been done entirely done without the use of generative AI. The files that have been used for this work are available on https://github.com/MartinBrans/PPG-Heart-Rate-Tracking and https://github.com/MartinBrans/MAX30101WING-Heart-Rate.

Chapter 1
Identification of Variables to Monitor

This chapter aims to overview the many tools and equipment used for firefighting (and search and rescue), and to identify what technologies (in the field of electronics, in the case of this work) could be considered to improve firefighter safety and efficiency. First, the most common equipment is presented to contextualise how the firefighter is protected against the most present dangers, typically fire, heat and smoke. Then, some modern variants and additions are presented and their features are explained, with a strong focus on electronics. This shows what is already possible to do, and what could be improved or added. Finally, a set of variables to monitor is established with the help of scientific literature and the experience of firefighters. Each variable is evaluated qualitatively, both in terms of relevance and feasibility. Different measuring techniques are presented and compared qualitatively to assess the latter.

1.1. Basic protective equipment for firefighting

In order to intervene safely on the site of the emergency, firefighters throughout the world employ PPE that consists of a fireproof suit, a helmet and an SCBA. This has been the most common set of equipment in use for decades, although the design of each piece has evolved greatly since.

First, the fireproof suit, such as the one represented in Figure 2, consists of a jacket, trousers, gloves and boots. Together, they offer insulation from the high temperature environment, so that the firefighter avoids burns from radiant heat, flames, hot surfaces, steam or others. They accomplish this by delaying the rise in temperature inside the suit as much as possible. For this purpose, different layers of fire-resistant fibres are combined to have a high heat capacity, mechanical strength and thermal stability, and a low thermal conductivity. These fibres must also allow the transfer of sweat to the outside, since the firefighter's physical efforts generate a lot of heat that must be dissipated via sweat. These suits must follow quality standards that depend on the region of use [16], [17].

Next, the helmet protects the firefighter's head from collisions with, e.g., falling objects or building structures. In some cases, it serves as an attachment point for the face mask

Figure 2: Jacket and trousers of a firefighter suit by Sioen Firefighter Clothing [17].

of the SCBA, or other equipment (a flashlight, for example). The firefighter's head is protected from the heat by a fireproof hood. The helmet can also hold a piece of fireproof cloth hanging from the back to further protect the neck. Examples are shown in Figure 3.

Finally, the SCBA allows the user to breathe clean air for about half an hour in environments with a low oxygen concentration and/or toxic substances (typically carbon monoxide and other incomplete combustion products). This system consists of an air tank, a pressure regulator, a pressure gauge, a lung demand valve and a face mask. An example is shown in Figure 4. The air tank is filled with regular air (not pure oxygen) at a pressure of a couple hundreds of bars and is worn on the back using backpack straps. The pressure regulator, beneath the tank, reduces the intake pressure of the system to a couple bars. Then, the valve, attached to the front of the face mask, feeds the clean air to the firefighter when they inhale, using a spring-loaded mechanism. The mask is pressed on the user's face, either using springs or straps that are attached to

(a) Fire hood PartX™ by Viking [18]. *(b) Gallet F1 XF helmet by MSA with an SCBA face mask attached [19].* *(c) Gallet F1 XF helmet by MSA with neck protection [19].*

Figure 3: Head protections for firefighting.

Figure 4: Dräger's PSS® AirBoss SCBA [12].

the helmet (see Figure 3(b)), or with straps that go around the back of the head under the helmet (see Figure 4). This creates a sealing between the user's face and the environment. The valve's mechanical system lets air pass when the pressure inside the mask decreases, i.e. when the user's lungs pull air in. Most of the time, the SCBAs used in firefighting are an open circuit. In that case, when the user breathes out, air leaks between the mask and the user's skin due to the excessive pressure. This is why the sealing created by the mask must be carefully designed: the outside air must not get in the mask when the user breathes in, but the stronger the sealing is, the more difficult it is for the user to exhale. SCBAs thus do not provide a perfect isolation of the air outside from the air the user breathes [13]. Alternatively, the user can press on a panic button to lock it in a position where air flows in (and out) continuously. This is because breathing with an SCBA demands a small but constant effort [1], so it is good to be able to breathe without restrain using this feature. However, the panic button consumes air at a much faster rate, so it should only be used when necessary, e.g., in case of exhaustion or panic. Lastly, the pressure gauge allows the user to monitor the pressure inside the tank, and thus the time remaining before a refill is necessary. Naturally, the duration mainly depends on the number of carried air bottles (usually one, sometimes two), their volume and initial pressure and the consumption of the user.

1.2. Capabilities of modern firefighting equipment

Electronics have already been integrated to commercially sold firefighter PPE and tools in many ways and are now increasingly present to assist in sensing, monitoring and communicating. In 2015, the USA's NIST reported on many potential improvements to firefighter PPE to be made in the near future in order to achieve "smart" firefighting

[13]. The following section aims to give a few examples of existing so-called “smart” PPE and tools, but these do not form an exhaustive list of possibilities, as many new products are on the horizon.

Voice telecommunication using radios is now very common in firefighting, just like in many other applications (the police, the industry, the military, etc.). Indeed, such a feature is very useful for many tactical reasons [13]. Both Dräger’s and MSA’s latest face mask have been designed to easily integrate a microphone and a speaker for that purpose. This add-on can then be connected to the radio with a cable [20], [21]. An example is given in Figure 5. Furthermore, communication between disciplines, i.e. between fire departments, emergency medical services, police departments, dispatching services, etc., has been studied to become more efficient. This has implied the installation of new infrastructure and equipment for first responders to coordinate themselves, such as ASTRID’s telecommunication services for first responders in Belgium. Since 1998, this state-owned company is responsible for developing and operating a network dedicated to communications between emergency services, offering voice telecommunication and text messaging via specialised radios and pagers. Their current focus is now on renovating the network with a wider band to allow for the larger data flows of IoT applications, using 4G/5G technologies [22].

In addition, excessive noise is an issue that has been overlooked for some time: some studies have concluded that firefighters are a population particularly at risk of suffering from noise-induced hearing loss [23], although others have found that the average exposure is below the recommended levels for common firefighting tasks [24]. The common sources of exposure are sirens, water pumps, saws, alarms, engines and radios. The simple solution to this problem when it arises is to wear adequate auditive protection when possible (e.g., outside of search and rescue tasks), but this protection tends to be underutilised. The causes of this behaviour are multiple, but they include the fact that communication and situational awareness are prioritised over hearing protection [25]. In that case, firefighters can opt for protective headsets equipped with wireless communication capabilities, such as the FHW507 headset from Firecom [26].

Figure 5: MSA’s C1 communication module for the G1 mask [21].

Dräger's PSS® AirBoss SCBA and its accessories have been briefly presented in the Introduction. Its features are very similar to MSA's M1 SCBA, hence why they are compared hereafter [12], [27]. The primary purpose of the device worn on the shoulder is to serve as a personal-alert safety system (PASS): it is meant to alert the other members of the team when it detects that their user might need help. PASSes usually achieve this by detecting the absence of movement for an extended period of time (e.g., 30 seconds) via tilt and/or acceleration sensors, by reacting to the press of an emergency button, or even in some designs by detecting excessive temperature. They then emit bright lights and loud sounds to help the teammates locate the firefighter in need of help. However, they are sometimes insufficient to prevent firefighter death or injury because they are used when the situation has already become an emergency [14]. The M1′s free fall detection feature aims to tackle a part of this problem by immediately detecting the dangerous free fall with a 1.5m threshold. Indeed, trips and falls represent a great risk in firefighting, so their automatic detection is of interest [14].

Air tank pressure is shown on the PSS® AirBoss/M1 control module, and the remaining duration of the breathable air supply is computed using this measurement. The module's battery (and additional electronics) is placed on the backplate, between the air tank and the back of the firefighter, and its charge is monitored as well.

These devices are then able to wirelessly communicate the information they gather to an entry management system, such as the Dräger FireGround or the MSA FireGrid. The entry management system collects the data sent by all the connected equipment on site, stores it on a cloud storage and streams it in real time to a central device (a tablet, such as in Figure 1(b), or a PC). A supervisor can then monitor their team in real time during interventions, and analyse the stored data afterwards, e.g., for performance assessments. Evacuation orders can be transmitted via the same wireless connection in case of immediate danger (e.g., risk of explosion, flashover, etc.) [28]. Both these systems use the LTE/LTE-M cellular network to connect the devices together. Repeaters can be deployed and extend the range of communication between devices, such as the MSA HUB [27]. The PSS® AirBoss is also equipped with Bluetooth and RFID interfaces for transferring recorded data [12].

Another technology that has integrated the firefighter's toolkit is thermal imagery. Depending on the conditions of the emergency, the visibility on the site can be extremely low, most often because of smoke accumulating in poorly ventilated areas [13]. According to Captain Lorent, one can sometimes not even see their hand if they hold it in front of them because of the smoke and lack of lighting. Thermal imaging cameras aim to help in these cases where search and rescue operations are very difficult and dangerous. They often come in the form of handheld devices, such as those shown in Figure 6 [29], [30]. However, some recent models now include the display directly in the SCBA's face mask, such that the firefighter can see the feed in a corner of their field of

(a) Dräger UCF® FireVista [29].

(b) MSA LUNAR [30].

Figure 6: Examples of handheld thermal imaging cameras.

view. This is the case of the Dräger UCF® FireCore, shown in Figure 7 [31]. Additionally, some cameras feature edge detection to make the monochromatic output more intelligible, such as the MSA LUNAR (Figure 6 (b)). Qwake has recently been developing C-THRU, a system that uses thermal imagery, artificial intelligence for edge detection, an augmented reality heads-up display, footage streaming for monitoring and footage recording for post-event analyses, among other features. Early tests showed significant improvement in the firefighters' ability to pass test scenarios. Although fire departments can sign up for a demonstration, this technology has yet to be turned into an industrialised product [32].

Lastly, knowing the exact position in 3D space of each firefighter is a very valuable information: if a critical problem were to happen to one of them, this information can drastically reduce the time lost rescuing the firefighter. It is also very useful for tactical decisions. At first, one might think about using satellite localisation. However, satellite coverage is not guaranteed, especially in buildings and underground infrastructure, and its accuracy is limited [13]. The MSA LUNAR's approach is to use relative positioning, in

Figure 7: Dräger UCF® FireCore thermal imaging camera and heads-up display [31].

the sense that it can show in which direction the other LUNAR devices are and approximately how far, although this information is not (yet) used to derive a more global robust positioning system [30]. The system developed by Chong *et al.* [33] is an example of how the global position of the firefighters can be derived by making them wear a device with a few sensors, without needing base stations. They achieve this using self-positioning information from regular sensors (an inertial sensor, a magnetometer, a barometer and a satellite positioning module) and mutual ranging with an ultra-wide-band radio sensor on each device. They found that this cooperative localisation performs better than with only the self-positioning sensors. Another approach is to bring reference emitters on site, and make the devices derive their position from the signals they receive. This is the approach of POINTER, developed in the USA by NASA's Jet Propulsion Laboratory and the DHS's Science and Technology Directorate. POINTER works based on a magnetoquasistatic field generated by a base emitter brought on site. The low-frequency magnetic field passes through most construction materials, unlike radiofrequency waves that can be blocked or reflected by them. The devices worn by the firefighters can then use this field to track their position in 3D throughout a building [34]. Neither of these two systems have yet been commercialised.

1.3. Identification of relevant variables

Now that a clear picture has been drawn on what features are found in commercial firefighter equipment, different variables can be identified as interesting to add to these features. Overall, vital signs are usually not part of the monitored features on connected PPE. As explained before, a modern PASS can detect some emergency situations, but not all, or sometimes too late. This is one of the reasons why this work is interested in vital signs monitoring, as explained in the Introduction.

Table 1 summarises all the variables that were considered thanks to a scientific literature review. The main articles driving the search were the review of vital signs monitoring for firefighters by Taborri *et al.* [1] and the NIST's research roadmap for smart firefighting [13]. The relevance of each potential feature is evaluated and justified using scientific literature and the experience of Captain Lorent. This is summarised in the table as well. At this stage, practical feasibility is not considered.

In this table, multiple vital signs are highly correlated with stress (be it psychological or physiological, or both), which makes them relevant. This is the case of heart rate (HR), breathing rate (BR) and body temperature, so there should be opportunity for redundancy, i.e. for an analysis that is robust to sensor noise. Hydration is also important to monitor, since its mismanagement can affect the firefighter in many ways. Some variables, such as heart beat patterns and VO2, can be analysed after the intervention to evaluate the firefighter's fitness and create individual fitness training programs, or recommend specific medical evaluations, for example [1]. In addition, the data collected

Objective	Variables	Relevance	Justification
Vital signs: Assessing the condition of the firefighter to manage their stress and exhaustion and evaluate their fitness.	Heart rate (HR)	High	Correlated with psychophysiological stress [2].
	Irregular heart beats	Medium	Early signs of long-term cardiac diseases [35].
	Breathing rate (BR)	High	Correlated with physiological stress [1], [36], [37].
	O_2 volume consumption (VO2)	Medium	Limited by SCBA [36], good fitness metric [1].
	Body temperature	High	Affects HR, hydration and performance [1].
	Hydration	High	Affects temperature, HR and performance [3], [38], [39].
Injury: Detecting signs of physical injury.	Trips and falls	High	Very common and dangerous [14].
Environment: Obtaining information on the environment that is relevant for tactical decisions.	O_2 concentration	Medium	Backdraft prevention [13], but they are preventable with training.
	CO concentration	Low	Toxic [13], but always present.
	Combustible gases	High	Detection of risks of explosion.
	Toxic substances	Low	Commonly encountered toxic particles [13], but preventable with an SCBA.
	Ambient temperature	Medium	Detection of flashovers [13], recognisable with training.

Table 1: General objectives, considered variables and their evaluated relevance.

overall could then be used for academic studies and surveys, to better understand the causes and impacts of stress on firefighters and adapt the intervention methods and training programs accordingly [2].

Moreover, when checking the activity of the firefighter, it would be interesting to detect trips and falls early instead of detecting their consequences. Indeed, they are a very common source of firefighter injuries, because of the poor visibility and unstable building structures.

Regarding environmental variables, the presence of flammable gases can present a risk of explosion. This has many implications on the tactics employed by the team, so measuring their presence and their concentration (to detect explosive air-fuel mixtures) is relevant. For the other gases, the opinions of the NIST's report and of Captain Lorent differ. On one hand, regarding carbon monoxide and other toxic gases, it is argued that their presence in the ambient air is inevitable, that SCBAs tackle this problem quite efficiently (and their condition is regularly checked), and that the remaining exposure should be no reason not to uphold the mission. The potential loss of life and property damage for the victims is simply a far worse consequence. Additionally, if the exact concentration needs to be known, emergency medical services often are able to provide equipment for that purpose. Still, the implementation of toxic substance sensors inside the SCBA could be interesting for studying the firefighter's exposure to these chemicals in the context of occupational health surveys. On the other hand, regarding oxygen concentration, the NIST's report states that monitoring it could help detect the conditions for a backdraft. A backdraft (or backdraught) occurs when the interior of a closed room has undergone partial combustion, but the combustion has slowed down because of a lack of oxygen. In these conditions, the room is very warm and full of flammable gases (because of pyrolysis), meaning the combustion only needs oxygen to go back to full strength. Then, if a door or a window to the exterior is opened, oxygen rushes in and flames violently blast out [40]. An oxygen concentration sensor could in theory warn the firefighter that they are in an oxygen-depleted room, so that they know windows and doors to the outside should remain closed. However, firefighters are already trained to recognise these cases and handle them, thus this feature is of lesser importance than at first glance. In a similar fashion, monitoring the ambient temperature could be of interest to predict flashovers. A flashover occurs when the materials in the environment are self-igniting because of the high temperature, creating a positive feedback loop and a sudden increase in temperature. This is because of pyrolysis, i.e. the creation of flammable gases due to high temperature. Additionally, the radiative heat from the hot smoke trapped by the ceiling feeds back to the fire, which reinforces the chain reaction. The fire can then very rapidly spread to other rooms. This effect happens under specific conditions that have been studied for a long time, and ambient temperature is a good way of predicting its appearance [41]. However, similarly to backdrafts, firefighters are trained to recognise when a flashover will occur, so measuring the ambient temperature is less relevant, although not completely irrelevant.

1.4. Measuring techniques and practical feasibility

Current technology offers different techniques to monitor the selected variables, with some that are better suited than others in the context of firefighting. Among the variables listed in the previous section, heart beat analysis (HR and heart beat patterns) and respiration analysis (BR and VO2) stand out in terms of practical feasibility in the context of this work. The others (body temperature, hydration, trips, falls and environment variables) have not been developed further in this work than the following summary for reasons explained hereafter.

Regarding the body temperature, the most direct technique is to measure the core body temperature. However, no non invasive practical techniques are known to measure this variable in the context of this work: either a probe is required to go inside the body, e.g., in the rectum or the oesophagus, or a telemetry pill has to be swallowed well in advance of the incident and recovered afterwards. Therefore, outside of academic studies using training scenarios, it is best to measure the skin temperature instead, and derive thermoregulatory strain from it [1]. In academia, skin temperature was measured on firefighters using different wearable sensor types: thermistors [42], infrared sensors [43] and on-chip sensors [44], [45]. These sensors are generally found on the market from basic blocks to advanced systems, including in commercial health-monitoring products. Integrating these solutions to firefighter PPE is left for other projects, due to a lack of time.

Regarding the hydration, bioimpedance analysis could potentially be used. A bioimpedance measurement is done by driving an AC voltage difference on two electrodes placed on the chest, and sensing the resulting current to derive the electrical impedance of the chest. Measuring the bioimpedance at different frequencies and over time gives useful information on the composition of the body, including hydration. However, there are still a few challenges to be solved to make reliable analyses from the measurements [46]. In addition, this technique suffers from practicality issues due to the use of electrodes. These electrodes can be covered with an electrolytic gel to increase their conductivity and make them sticky, but it makes them uncomfortable and too slow to put on (while response time is key in firefighting). If no gel is used, the electrodes are said to be dry, their impedance is much higher, and any slight movement relative to the skin causes a lot of noise. The relative movements can be mitigated thanks to the latest advancements in smart textile technology: the dry electrodes can be integrated into a flexible garment, and the electrodes are then capacitively coupled to the skin. Such a technique has been used in many studies for electrocardiography measurements (which uses the same type of electrodes) [2], [47], [48], and is becoming a commercially available solution for researchers and engineers. Shen *et al.* [49] have presented an example of electrodes in a fabric used for bioimpedance measurements, although respiration is the focus of their work, and not hydration. The alternative to bioimpedance measurements is an electrochemical sensor measuring the concentration of electrolytes in the sweat, which reflects the level of hydration of the user (high concentration means low hydration). These have recently received significant improvements, but challenges also remain in terms of reliability and power consumption [50]. A few commercial products exist for fitness and worker safety applications, including in the form of an arm band instead of uncomfortable skin patches that have to be replaced. In any case, the work to be done on the reliability of hydration monitoring is out of the scope of this work.

Regarding trips and falls, researchers have developed different approaches based on a combination of readily available sensors such as inertial sensors, barometers and magnetometers. Chai *et al.* [14] used a neural network for the processing of the data from an array of inertial sensors, while other studies have used a conditional approach, using thresholds for posture recognition and impact detection [51], [52]. On the market, simpler solutions can be found, such as the M1 SCBA's free fall detection feature presented before, also using inertial sensors [27]. The rest of commercially available solutions are designed for the elderly and patients with slow movement, which makes them unsuitable for the application [52]. The research to be done is also outside the scope of this work.

Finally, regarding the analysis of the environment, gas sensors and temperature sensors that can resist the environment of firefighting are easily found on the market of industrial safety equipment as portable devices, or as basic blocks from electronic component providers. Nascimento *et al.* [15] gave an example of how gas sensors can be integrated to firefighter PPE, although the system was not tested in real conditions and is not protected enough against the environment. The integration of these sensors into existing systems such as those seen in Section 1.2. is left to the firefighting equipment designers.

The remaining variables can be grouped into two categories: heart beats and respiration. For each category, a few measuring techniques are described and compared in terms of availability, integration and performance in their respective subsections. As a disclaimer, the actual performance of a system will highly depend on the subsequent design choices when developing the system, and not only on the chosen technique. This means that the qualitative comparisons presented here are not an absolute truth.

1.4.1. Heart beats

Table 2 summarises the comparison between three popular techniques for sensing heart beats:

- Photoplethysmography (PPG): measuring the changes in reflectivity of the skin due to blood and oxygen concentration variations with an LED and a photodetector.
- Electrocardiography (ECG): sensing the electric pulses of the heart using electrodes, either with or without electrolytic gel.
- Seismocardiography (SCG): recording the body-surface vibrations induced by the heart beat using micro-electro-mechanical systems. Also known as ballistocardiography.

Each of these techniques can be used to derive HR, as well as other variables if the signal is clean enough (because they are typically based on the patterns in the pulses). The summary table compares the different techniques on several aspects: availability of

Technique	Availability		Integration	Noise
	Hardware	Software		
PPG	■	■	■	◆
ECG w/ gel	■	■	●	■
ECG w/o gel	◆	■	■	◆
SCG	◆	●	■	●

Table 2: Comparison of wearable technologies for sensing heart beats on different aspects.

the hardware on the market (with cost taken into account), availability of the software on open-source software platforms or in academic papers, integration to firefighter PPE, and sensitivity to noise. A green square (■) means the technique is quite good on the corresponding aspect, an orange diamond (◆) means there are some hurdles that can be overcome, and a red circle (●) means there are major flaws that discourage the use of this technology in the context of this work.

PPG stands out because it is non invasive, cheap, popular and easily integrated into the PPE, even though it can be sensitive to crossover noise (typically artefacts caused by motion) [53]. The other techniques are more difficult to adapt to the context of this work. For ECG, the same problem observed for bioimpedance measurements appears again. Using gel on the electrodes makes ECG the gold standard in terms of accuracy in medical applications, but it makes them uncomfortable and too slow to put on. Dry electrodes can be integrated into a smart textile, but these materials are more expensive to obtain and develop, and the resulting signal can still be disturbed by motion artefacts [47]. In spite of this, studies have shown that ECG without gel can be used for HR monitoring in the context of physical activities [49], and even in firefighting [2]. Finally, SCG is a rather niche technique, and is inherently less suitable for physical activities (including firefighting) [54]. The inertial sensors can be integrated into textiles, similarly to electrodes. However, open-source signal processing software is harder to come by, and even more so for physical activities. This technique has rather been used in continuous health monitoring applications [55], [56], [57], or in non invasive medical diagnostics (often in conjunction with ECG) [58]. Some efforts are being made to make SCG signal analysis more robust to motion artefacts [54], but overall this technique is too complex to be employed in firefighting.

1.4.2. Respiration

Table 3 summarises the comparison between different techniques for analysing respiration:

- Bioimpedance analysis: observing the changes in impedance of the chest using electrodes, by driving an AC voltage and sensing the resulting current.

- Chest movement: measuring the displacement of the thorax with a sensor. The sensor can be a deformable antenna, an RFID/NFC sensor, a strain sensor (capacitive, resistive, piezoelectric, ...), an inertial sensor, etc. (see [37]).
- ECG/PPG/SCG: using PPG, ECG or SCG signals, BR can be computed because of its influence on the signal's baseline (low-frequency component) and on the frequency and amplitude of heart beats (see [59]).
- Modified SCBAs: the SCBA's lung demand valve can be modified to not only sense breaths, but also air volume consumption and VO2.

The same criteria and colour code as Table 2 are used for this table as well.

First, bioimpedance has the advantage of having a linear relationship with chest volume [60], but its measurement suffers from the same tradeoff between integration and noise sensitivity (and cost) that was discussed before. Shen *et al.* [49] have used this technique combined with ECG and SCG to derive BR, using sensor fusion. Other articles detail how to derive BR from bioimpedance measurements [61], [62]. Second, several types of sensors based on chest movements have been reviewed by Hussain *et al.* [37]. They come in a variety of forms, but they generally rely on the use of smart textiles or chest straps, and many are sensitive to the motion of the body. Third, deriving BR from ECG/PPG/SCG signals greatly reduces the cost of sensing both respiration and heart beats. The signal has to be clean enough for that matter, but many articles have shown how it can be done [49], [59], [63]. The performance reported in the table is that of PPG, since it was identified as the best technique in Section 1.4.1. Finally, SCBAs provide a unique opportunity to easily sense BR and air volume exchange, especially thanks to the lung demand valve and the pressure sensor. Some studies have also added a metabolic device (the Cosmed K4b2) to measure VO2 [64], [65]. The technique seems to be easy to develop, although it hasn't been tried many times in academia. Due to a lack of time, however, none of these techniques will be further studied in this work.

Technique	Availability		Integration	Noise
	Hardware	Software		
Bioimpedance	◆	■	■	◆
Chest movement	◆	■	■	◆
ECG/PPG/SCG	■	■	■	◆
Modified SCBA	■	■	■	■

Table 3: Comparison of wearable technologies for sensing respiration on different aspects.

1.5. Final selection and chapter conclusion

In summary, the possibilities for monitoring firefighter vital signs are numerous. Examples of complex systems presenting multiple health-monitoring features can be found in academia, including, but not exclusively, in the context of firefighting. Indeed, the field of fitness and health monitoring is developing many solutions that can be directly applied to firefighting. It also means many commercial products are already available. This is because any equipment placed underneath the suit will be as protected as the firefighter themselves, so the constraints on physical robustness are not much higher than in the context of sports and fitness. Researchers and engineers can therefore profit from advancements in both fields.

HR is the variable chosen to be studied in the rest of this work because of its high correlation with psychophysiological stress. Other variables were identified as interesting to add to multi-sensor firefighter PPE (especially respiration), but they are left for future work on this topic due to a lack of time. A lot more research has yet to be done for some of the technologies that were reviewed in order to improve their reliability, namely hydration monitoring and the detection of trips and falls (outside of monitoring elderly populations). Most measuring techniques were tested during basic physical activities (typically, running on a treadmill), but they still have to be tested in firefighting conditions.

PPG is the technique chosen to measure HR in this work because it is simple, non invasive and easily integrable to firefighter PPE. BR and other valuable metrics in occupational health can be also extracted from the PPG signal. In addition, it is rather cheap and readily available in many forms, from basic blocks and modular systems to fully developed products. It can be quite noisy because of external influences, especially motion artefacts, but the research on the topic is abundant, so there are ways to make it reliable. ECG is an interesting alternative, but it is more expensive and complex. The rest of this work thus attempts to find and test an open-source algorithm to embed into a sensor for a robust real-time processing of the raw PPG signal.

Chapter 2
Study on PPG-based Heart Rate Algorithms

Photoplethysmography (PPG) is defined as the detection of blood volume changes in the microvascular bed of the skin based on optical properties of the human body composition under a specific wavelength [66]. An illustration of this technique is shown in Figure 8. In a nutshell, a device emits light of a specific wavelength (usually green) and intensity on the skin, and some of the light scatters, reflects or gets absorbed by blood and tissue. The device then records the intensity of the light exiting the skin using a photodetector. When the heart beats, the amount of blood in the exposed skin varies slightly, which influences the intensity of the light sensed on the receiving end of the device. These intensity variations are seen as pulses on the recorded signal, which can be analysed to derive HR, BR, and more. In Figure 8(a), this scheme is done on the fingertip, but it can also be done on the earlobe or the wrist. In the following chapter, the latter will be the location used, with a reflectance configuration. This is because it can then be integrated into a bracelet, making the device compact, easy to design and comfortable to wear. The practical aspects will be further discussed in the following chapter.

In this chapter, different algorithms that extract the HR from the PPG signal are studied. First, various algorithms are explained and placed in three different categories.

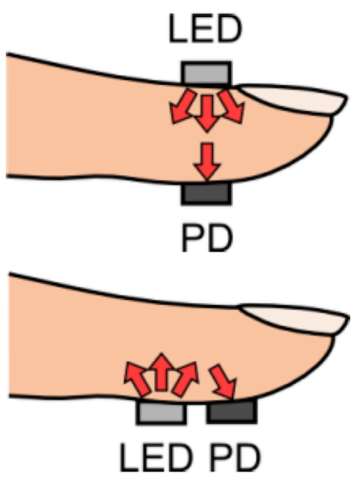

(a) Placement of the light-emitting diode (LED) and photodetector (PD) on the fingertip for transmission and reflectance mode.

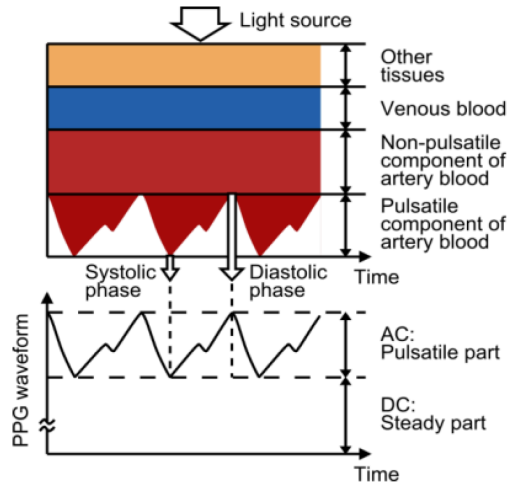

(b) Variation in light attenuation by tissue.

Figure 8: Illustration of the concept of PPG [67].

Then, the datasets that are used to compare their accuracy are presented. Finally, several comparisons in terms of accuracy are made to test different hypotheses. Since the application implies a lot of movement from the user, the robustness to motion artefacts receives a strong focus. Indeed, the movement of the device on the user's skin can cause changes in the different components of the signal, which is a form of crossover noise.

2.1. Presentation of open-source algorithms

The sources of the algorithms were mostly found on GitHub using keywords related to PPG and HR. Five sources have been found, from which a few other variants have been created to test different hypotheses. They have been sorted in three categories: spectrum-based, peak-based and threshold-based. The advanced signal processing techniques used in the scientific literature on this topic are briefly mentioned.

2.1.1. Spectrum-based algorithms

This category is based on the frequency spectra of the available signals, i.e. their discrete Fourier transform (FFT). The proposed Python HR algorithm was found in a GitHub repository from the IEEE Signal Processing Cup of 2020 [68]. An illustration is shown in Figure 9.

The PPG signal is first zero-padded to 4 times its length, and its spectrum magnitude is obtained using NumPy's `rfft` function. The zero-padding serves to have more samples of the spectrum that are closer to each other (although the resolution is not improved). The peaks in the spectrum are then identified using SciPy's `find_peaks` function. In the absence of motion artefacts, the frequency of the highest peak is converted in beats per minute (BPM) and the result is the predicted HR value. If there

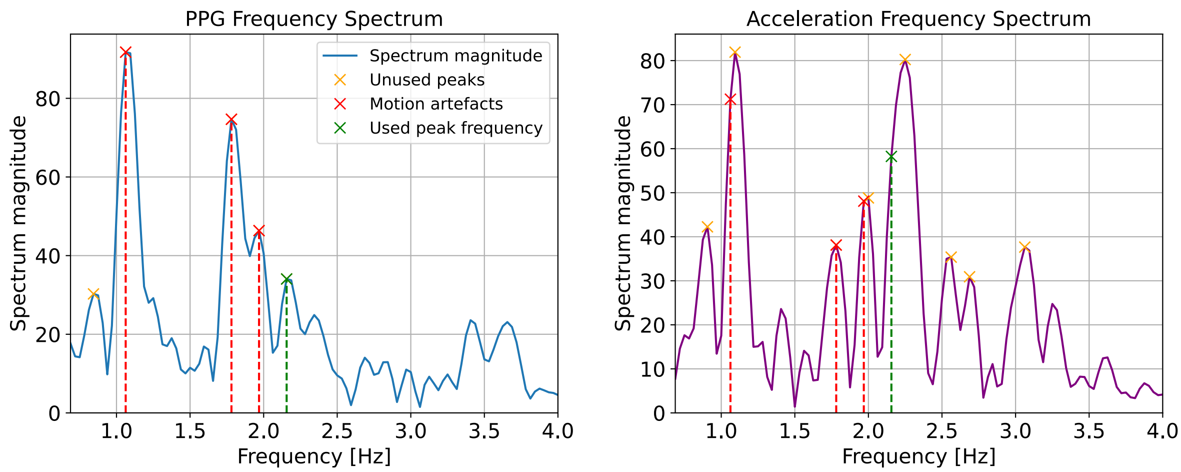

Figure 9: Application of the "FFT Peaks" algorithm on an example. The three highest peaks in the PPG spectrum are rejected because they are too close to peaks in the acceleration spectrum.

is motion, the accelerometer data is used to try to sort out which peaks are caused by motion artefacts. This is done by taking the magnitude of the acceleration vector thanks to the three accelerometer channels (one per axis), and locating the peaks in its frequency spectrum (using the same zero-padding and `rfft`). If the frequency of the highest peak in the PPG spectrum (or its two neighbouring frequencies) is also related to a significant peak in the acceleration spectrum, then it is considered a motion artefact, and the operation is repeated for the next-highest peak. This method aims to cancel periodic motion artefacts, e.g., those caused by arm movements when running. A variant was derived where the acceleration signal is ignored, to test whether taking it into account is beneficial for accuracy.

2.1.2. Peak-based algorithms

This category of algorithms is based on detecting peaks in the signal, i.e. times where the signal rises and falls quickly, creating a peak well above most of the signal. Assuming each peak corresponds to a heart beat, HR can be computed from the list of peak locations. This is the technique used by BIOBSS [69], a Python library for signal processing and feature extraction on biological signals. It can process ECG and PPG signals and extract features from them such as HR, HR variability metrics, BR and many more. BIOBSS also handles electrodermal activity and 3D acceleration signals, but there is no direct way to use the latter to remove motion artefacts from a PPG signal with this library alone.

Various methods exist to detect peaks in a PPG (or ECG) signal. BIOBSS' default method for peak detection is to run through the whole signal while switching between two modes: either looking for a local maximum, or for a local minimum. Figure 10 illustrates how the algorithm looks for a local maximum:

(1): A variable `MX` starts as the previous local minimum value.
(2): `MX` is updated to the signal's value when it goes higher than `MX`.
(3): If the signal goes lower than `MX` by a significant margin, the peak is found: the signal was increasing and is now decreasing. The mode is now switched to local minimum detection.

The local minimum detection mode works the opposite way, i.e. by looking for when the signal goes sufficiently above a decreasing value `MN`, that started at the latest `MX` value. The margin used to switch modes, `delta`, is to be defined by the user based on the amplitude of the signal. Alternatively, BIOBSS can detect beats by searching in the signal for rising edges. This is done by performing peak detection on the signal's first derivative, which is estimated using NumPy's `gradient` function. This feature will also be tested.

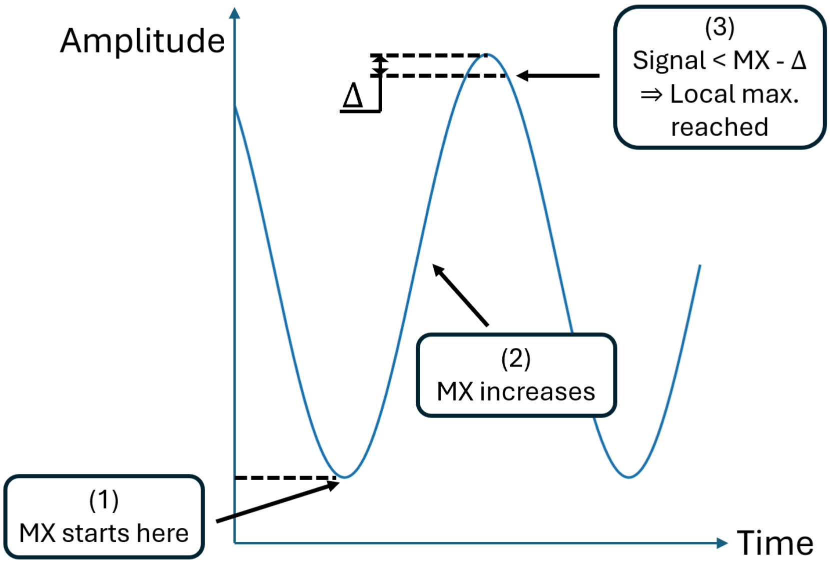

Figure 10: Illustration of BIOBSS' peak detection algorithm.

SciPy's `find_peaks` function is another popular method for peak detection on ECG and PPG signals. It works by listing every sample that is greater than its two neighbouring samples (ignoring the signal's edges). The user can then specify required peak properties to filter out the irrelevant peaks: minimum/maximum height and/or width, minimum horizontal distance between peaks, minimum/maximum prominence, etc. The parameters that are used in the experiments are minimum height and minimum horizontal distance. The former is fine-tuned to give the best accuracy, while the latter is set to space out the peaks by 0.3 seconds or more (which corresponds to a maximum HR of 200 BPM).

Finally, the MAX30101WING, the PPG sensor evaluation board used in the prototype of Chapter 3, comes with an open-source example code that is also based on peak detection [70]. It does so by looking for consecutive samples that are increasing. The peak is located at the first sample that is lower than the previous one, if the chain of increasing samples is long enough.

2.1.3. Threshold-based algorithms

This category of algorithms is based on beat/peak detection using thresholds. The first algorithm originates from two open-source learning projects by Tsai that use the MAX30102 PPG sensor and the MAX86150 ECG/PPG sensor respectively [71], [72]. It works by detecting when the signal passes through two thresholds, which is illustrated in Figure 11:

(1): Passing below the lower threshold for the first time triggers a `beatStarted` flag that activates the upper threshold.

(2): Passing above the upper threshold with the `beatStarted` flag raised triggers a `beatComplete` flag.

(3): Passing below the lower threshold again with the `beatComplete` flag raised marks the end of the beat, the length of which is the time difference between steps (1) and (3). The `beatComplete` flag is reset.

The `beatStarted` flag is important for the first beat only, after which it stays raised. At the beginning of the run, if the signal passes above the upper threshold then below the lower threshold (see (!) in Figure 11), completing a beat, there is no way of knowing when the beat started. It could have started at any time before the first sample. Therefore, the first beat has to be inside the window from its beginning to its end, otherwise it won't count. The two thresholds are defined using the maximum and minimum values of the signal.

The two thresholds of Tsai's algorithm, although adapted to the signal's amplitude using the extrema, are set quite arbitrarily. In contrast, the HeartPy Python library has a method of adapting its single threshold to find the best fit, using a moving average and a hyper-parameter. Its method is based on peak detection, where consecutive samples above the threshold are considered part of a peak, and the peak is located using the maximum value of the continuous segment above the threshold. The threshold is calculated by adding a percentage of the mean of the signal to the moving average. Several percentage values (the hyper-parameter) are tried in order to find the one that minimises the variance of the time difference between peak locations. An illustration is given in Figure 12. HeartPy is also capable of post-processing these peaks to remove outliers that are oddly spaced out compared to the others. Further details and features are explained in the associated articles by van Gent *et al.* [73], [74].

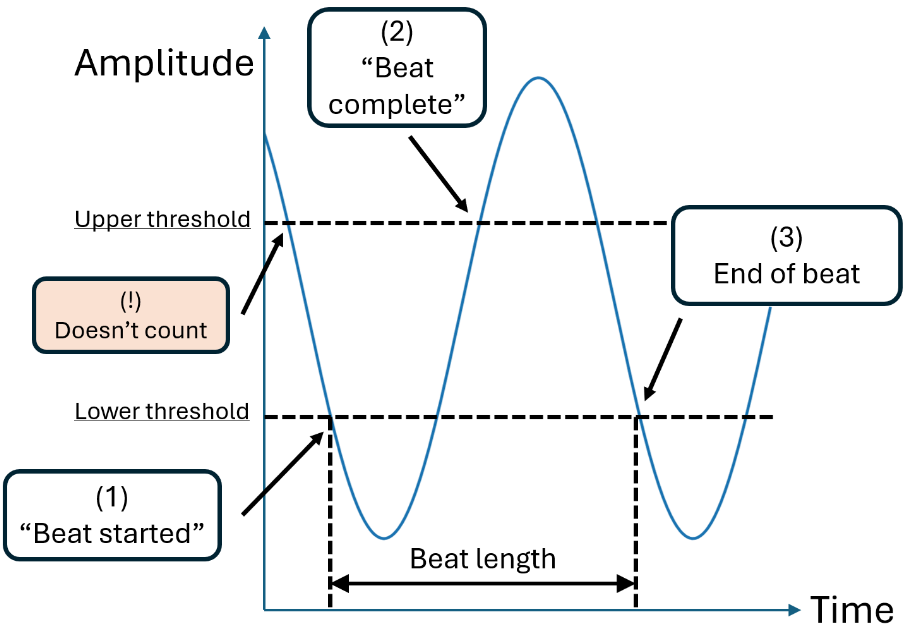

Figure 11: Illustration of the two thresholds algorithm by Tsai.

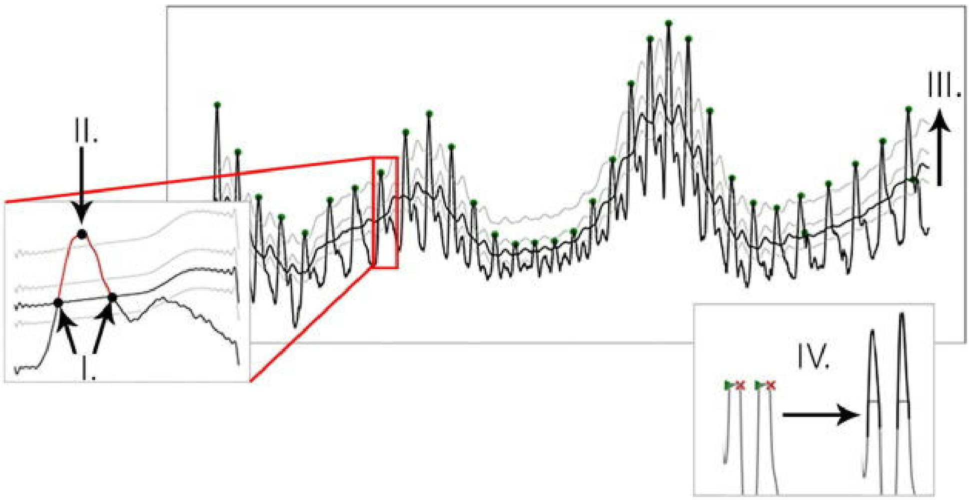

Figure 12: Illustration of the HeartPy peak detection algorithm [74]. The segment of the signal in red is above the variable threshold (smoother black line), and the corresponding peak is located at its maximum value (II.) The light grey lines represent the different thresholds tested.

2.1.4. Converting peaks and beats to heart rate

Once the peaks (or beats) are located, there are different approaches to compute HR. For example, HeartPy and BIOBSS convert the mean time between peaks in BPM, while Tsai's and the MAX30101WING example code use the mean of the HR values computed beat-to-beat. To test whether this has an impact on accuracy, four variants have been created where peaks are found using SciPy's `find_peaks` function with the same parameters (height and distance, which were manually tuned to minimise the mean absolute error on both datasets), and the HR value in BPM is computed in four different ways:

1. HR is the number of peaks divided by the length of the window in minutes.
2. HR is the inverse of the mean interval in minutes between two consecutive peaks (HeartPy, BIOBSS).
3. HR is the mean of the HR values computed using consecutive peaks (Tsai's, MAX30101WING).
4. HR is the median of the HR values computed using consecutive peaks.
5. HR is the inverse of the mean interval in minutes between two consecutive peaks, after removing the intervals with an absolute Z-score above 2.

The fourth and fifth approach are designed to be more robust to misidentified peaks that would significantly influence the mean performed in the second and third cases. Note that the reference HR in both datasets is computed using the second approach (applied to the ECG signal), so the experiment will be biased towards it in theory. Still, the impact of this choice is interesting to measure.

2.1.5. Algorithms from the scientific literature

A lot of advanced techniques exist in the scientific literature to process PPG signals in a robust manner. Ismail *et al.* [75] reviewed some of the best examples of PPG signal processing techniques in terms of robustness against motion artefacts, which is of great interest for this work. They decomposed the algorithms in two steps: the removal of motion artefacts and the HR tracking. They then categorised several approaches for each step. The motion artefact removal can be made with adaptive filtering, signal decomposition, or other techniques. The HR tracking is based either on signal decomposition, signal subspaces, signal processing or machine learning. Among the reviewed algorithms is the one developed by Zhang *et al.* [76], the creators of the TROIKA dataset. It uses signal decomposition, sparse signal reconstruction and spectral peak tracking. Unfortunately, the implementation of this algorithm is not open-source, nor are those of most of the algorithms reviewed by Ismail *et al.*. Implementing them using the details in the articles would take too much time, but their accuracy is known, so they can still be compared to the other algorithms in this chapter. Finally, Temko [77] developed an open-source algorithm in MATLAB. It hasn't been re-implemented in Python for this work due to a lack of time, but its performance on the TROIKA dataset are detailed in the associated article.

2.2. Datasets

In order to evaluate the accuracy of the studied algorithms, two publicly available datasets are used:

- The first is a subset of the CapnoBase IEEE TBME Respiratory Rate Benchmark [78], [79], a dataset for respiratory rate estimation from PPG signals. This dataset contains recordings of high-quality PPG and ECG signals that were sampled at 300 samples per second, as well as reference HR data. The ground truth HR ranges between 50 and 150 BPM. Signal peaks caused by heart beats and motion artefacts were manually annotated by experts for both channels, and the ECG channel is used to derive the reference HR. This dataset serves to confirm the correct behaviour of the algorithms in ideal conditions (when crossover noise is negligible), and to select the algorithm that generates the least absolute error on average. The recordings overall contain very few motion artefacts, and some don't contain any at all. Out of the 42 recordings of 8 minutes available in the online database (5.6h in total), 15 recordings (2h) were used for this work, which were selected because they had no reported motion artefacts on the PPG channel. This is to guarantee that they had no influence on the reported accuracy. 13 additional recordings (1.7h) with a few artefacts have also been downloaded for a separate experiment.
- The second dataset is the TROIKA dataset, designed for the benchmarking of algorithms on PPG signals with a lot of motion artefacts [76]. It contains recordings of

a wrist-worn device with a PPG sensor and a 3-axis accelerometer. Reference HR values, ranging from 65 to 180 BPM, are pre-computed from an ECG signal, which is also provided. There are 12 5-minute-long recordings with a sampling frequency of 125 Hz. While the dataset is no longer available directly on the author's site, a copy was found on a GitHub repository by Strand from the IEEE Signal Processing Cup of 2020 [68] (which also provided the spectrum-based algorithm). This dataset is used to show the influence of motion artefacts, and why having a strategy to deal with them is crucial.

The distribution of ground truth HR in both datasets are shown in Figure 13. For CapnoBase, the selection of recordings without artefacts has biased the ground truth HR towards 70 BPM. This is deemed acceptable still, since experiments on the 13 additional recordings with artefacts have given similar results as on those without artefacts. The distribution of ground truth HR in these noisier recordings is shown in Figure 22 of Annex A, and it is better balanced. The distribution in the TROIKA dataset leans slightly towards high HR values, around 150 BPM.

The experiments use TROIKA's format of estimating HR in beats per minute (BPM) on an 8-second-long window of the available signals. Most of the algorithms have parameters that can be tuned based on, e.g., the signal's amplitude. In order for the algorithms to have a single set of parameters that works on both datasets, a preprocessing step is added. The PPG signal window first goes through a third-order band-pass Butterworth filter with cutoff frequencies of 0.67 Hz (40 BPM) and 4 Hz (240 BPM). These frequencies are far enough away from the expected heart rate values, so as to not cut them off. The result is then normalised with the standard deviation of the filtered signal. In the case of the acceleration, the filtering of the Y-component (in the vertical direction) is skipped to preserve the component due to gravity. The filtered acceleration vector magnitude is thus obtained by applying Pythagoras' theorem to the

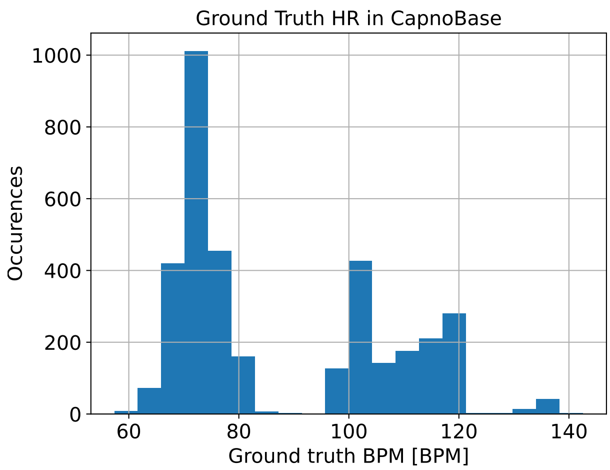

(a) CapnoBase

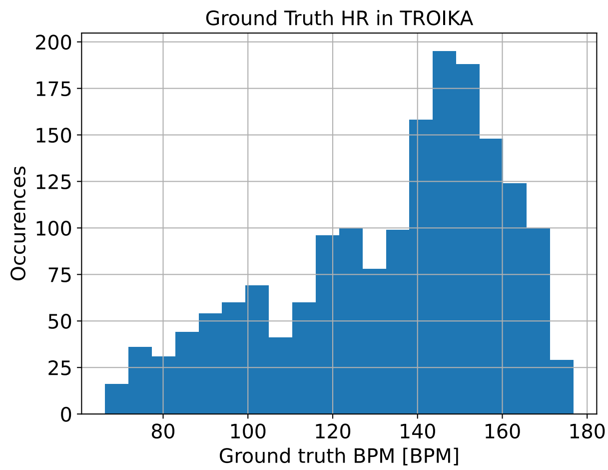

(b) TROIKA

Figure 13: Distribution of ground truth HR values in the datasets.

filtered X- and Z-components, and the unfiltered Y-component. The result is then filtered to remove some of the noise of the Y-component, and normalised. Unfortunately, the preprocessing step did not fully remove the dependency of the optimal parameter values on the dataset, so a compromise has been found instead to have good accuracy on both with a single set of parameter values.

2.3. Comparison of algorithms in terms of accuracy

The algorithms presented in the previous section were compared on the two datasets (CapnoBase and TROIKA) by giving them a series of 8-second windows of the PPG and acceleration signals. Two consecutive window in the same recording overlap each other by 6 seconds. Since the CapnoBase dataset doesn't have acceleration data, a null signal was given instead. This is acceptable because the CapnoBase dataset was chosen to test algorithms in ideal conditions, and the recordings were chosen to contain no motion artefacts.

The two metrics commonly used to compare the accuracy of HR-tracking algorithms in the scientific literature is the mean absolute error (MAE), in BPM, and the mean absolute percentage error (MAPE), in percents. They are also often called Error1 and Error2, respectively. They are defined as:

$$\mathrm{MAE} = \frac{1}{N} \sum_{i=1}^{N} \mid \mathrm{HR}_{\mathrm{pred},i} - \mathrm{HR}_{\mathrm{true},i} \mid \tag{1}$$

$$\mathrm{MAPE} = \frac{100}{N} \sum_{i=1}^{N} \frac{\mid \mathrm{HR}_{\mathrm{pred},i} - \mathrm{HR}_{\mathrm{true},i} \mid}{\mathrm{HR}_{\mathrm{true},i}} \tag{2}$$

where N is the number of windows on which an algorithm is evaluated, and where $\mathrm{HR}_{\mathrm{pred},i}$ and $\mathrm{HR}_{\mathrm{true},i}$ are the predicted and ground truth HR values of the i-th window, respectively.

2.3.1. In ideal conditions

The first comparison made is of the three different categories that were presented (spectrum-based, peak-based and threshold-based) in ideal conditions. This was done on the CapnoBase dataset, which is free of motion artefacts. A dummy algorithm has been added for comparison, which outputs a random number with a uniform distribution between 50 BPM and 150 BPM (the minimum and maximum of the reference HR across the whole dataset, respectively). The results are shown in Table 4. The majority of algorithms have yielded excellent results in this experiment, with MAE below or near 0.5 BPM. The MAE of Tsai's algorithm is higher but still decent, below 2 BPM. In comparison, the algorithms reviewed by Ismail *et al.* [75] showed MAE between 0.74 BPM and 3.75 BPM, although they used significantly noisier data and more advanced

Category	Name	MAE [BPM]	MAPE [%]
Spectrum-based	FFT Peaks [68]	0.563	0.686
Peak-based	BIOBSS Peaks [69]	0.294	0.379
	BIOBSS Beats [69]	0.228	0.277
	SciPy `find_peaks`	0.363	0.472
	MAX30101WING [70]	26.907	34.337
Threshold-based	Tsai [71], [72]	1.398	1.760
	HeartPy [73], [74]	0.227	0.285
Dummy	Random (50–150 BPM)	29.672	36.088

Table 4: Accuracy of the main concepts on the CapnoBase dataset.

techniques. This shows that each approach (spectrum-based, peak-based and threshold-based) can work in these ideal conditions. The MAE of the spectrum-based algorithm is slightly higher than the others', which could be due to the limited spacing of the frequencies (1.875 BPM). This is noticeable in Figure 14. Increasing the zero-padding helps, up to an extent (see Figure 23 in Annex A). Finally, the MAX30101WING example code performed similarly to the dummy algorithm, which means it didn't work at all. It is suspected that a problem occurred during its evaluation, but the problem could not be found despite many efforts. The fact that the code is very long and very poorly maintained, with very few comments, poorly named variables, unused/inefficient pieces of code and no sources, hinders greatly the debugging process.

Next, the impact of the HR calculation method is shown in Table 5. As a reminder, the different methods to compute HR from a list of peaks/beats information were explained in Section 2.1.4. In this experiment, the peaks were obtained using SciPy's `find_peaks` function. As expected, using the mean of the intervals between peaks yields slightly better results, and even more so when intervals with a poor Z-score are removed, because it is the method used to define the reference HR. Averaging the HR values is

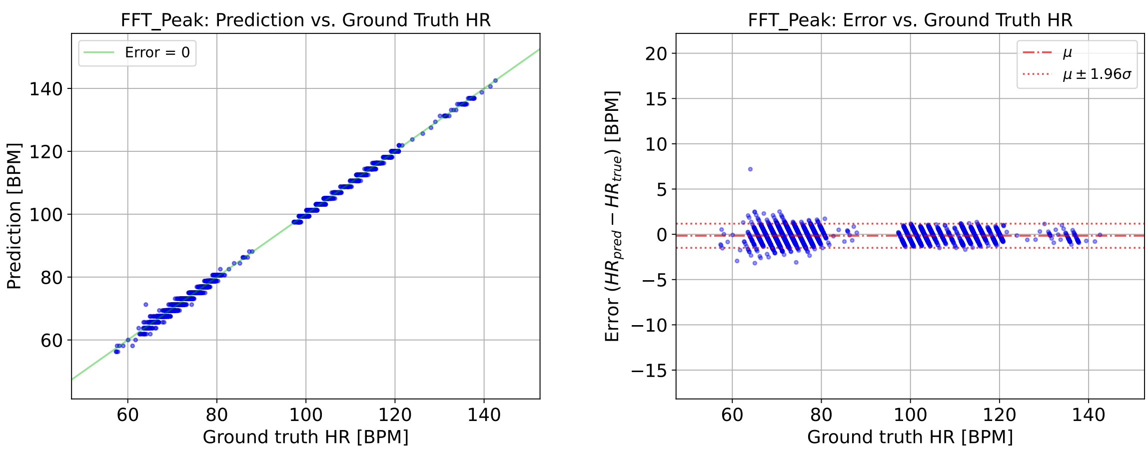

Figure 14: Predicted HR and error over ground truth HR for the spectrum-based algorithm on the CapnoBase dataset. The mean and 95% confidence interval of the error is also shown.

Method	MAE [BPM]	MAPE [%]
Number of peaks	2.745	3.336
Mean of intervals	0.363	0.472
Mean of HR values	0.555	0.746
Median of intervals	0.471	0.584
Mean of intervals w/ $\|z\| < 2$	0.234	0.291

Table 5: Impact of the HR calculation method on accuracy.

slightly more sensitive to the outliers. The error when taking the number of peaks is much higher likely because the 8-second-long window is rather short and contains only a handful of peaks. This means the resolution is not great. For example, at 100 BPM of ground truth HR, we should see 13 beats, which gives an estimate of 97.5 BPM based on this method. If we find 14 beats, we have an estimate of 105 BPM. A similar problem arises when using the median, because the limited resolution caused by the limited sampling rate likely has an influence on the error. At 100 BPM of ground truth HR, if the median is longer by just one sample (1/300 s, i.e. 3.33 ms), it creates a difference of 0.55 BPM. With Tsai's peak detection method, using the Z-score is also the preferred method, but not with BIOBSS and HeartPy. This is likely because they already have mechanisms to remove outliers and minimise interval variance. In their case, taking the mean of all intervals is the best choice.

2.3.2. In the presence of motion artefacts

The third comparison is made using the TROIKA dataset and the best-performing algorithm of each category, or "best performers" for short. The dummy algorithm has been adapted to the maximum and minimum reference HR values in this dataset. The results are shown in Table 6. They are drastically worse than in the ideal case, beyond what would be acceptable for a HR monitoring device. This shows how the impact of motion artefacts cannot be neglected. In comparison, Temko's algorithm [77] presented error rates that were much lower on the same dataset, with an MAE of 2.95 BPM. Its performance is shown in Figure 16. The best performing algorithm is the spectrum-based, thanks to the fact that it uses the accelerometer signal to filter out some of the motion artefacts. Removing that feature increases its MAE to 21.72 BPM and its MAPE to 16.59%, which is comparable to the others. Its performance is shown in Figure 15.

Category	Name	MAE [BPM]	MAPE [%]
Spectrum-based	FFT Peaks [68]	16.338	12.559
Peak-based	BIOBSS Beats [69]	18.982	16.853
Threshold-based	HeartPy [73], [74]	20.115	15.232
Dummy	Random (65–180 BPM)	43.024	31.740

Table 6: Accuracy of the best performers on the TROIKA dataset.

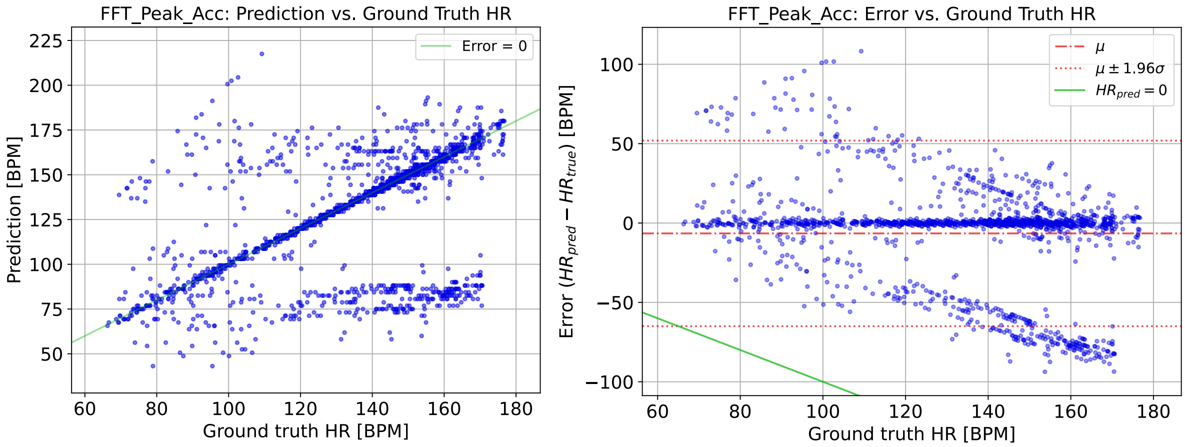

Figure 15: Predicted HR and error over ground truth HR for the spectrum-based algorithm on the TROIKA dataset. The mean and 95% confidence interval of the error is also shown.

To test whether this loss in accuracy is due to the reduced sampling frequency of this dataset (125 Hz instead of 300 Hz), another experiment has been done using the CapnoBase dataset with the PPG signal interpolated at 125 Hz. The results are shown in Table 10 in Annex A. The error barely increases for most, although “BIOBSS Beats” is slightly more affected due to the fact that it depends on the first derivative of the signal (retuning the hyper-parameter would probably help). Overall, this shows that the sampling rate is not the source of errors when testing on the TROIKA dataset. As mentioned before, the parameter selection has been initially tuned to yield decent results on both datasets at the same time. Among the best performers, this applies only to BIOBSS Beats, since the `delta` parameter has to be manually tuned. FFT Peaks isn’t affected much, while HeartPy has mechanisms to adapt its parameters on the fly. If BIOBSS’ `delta` parameter is fine tuned for an optimal performance on the TROIKA dataset, it results in a MAE of 17.29 BPM and a MAPE of 14.29%, which isn’t much better.

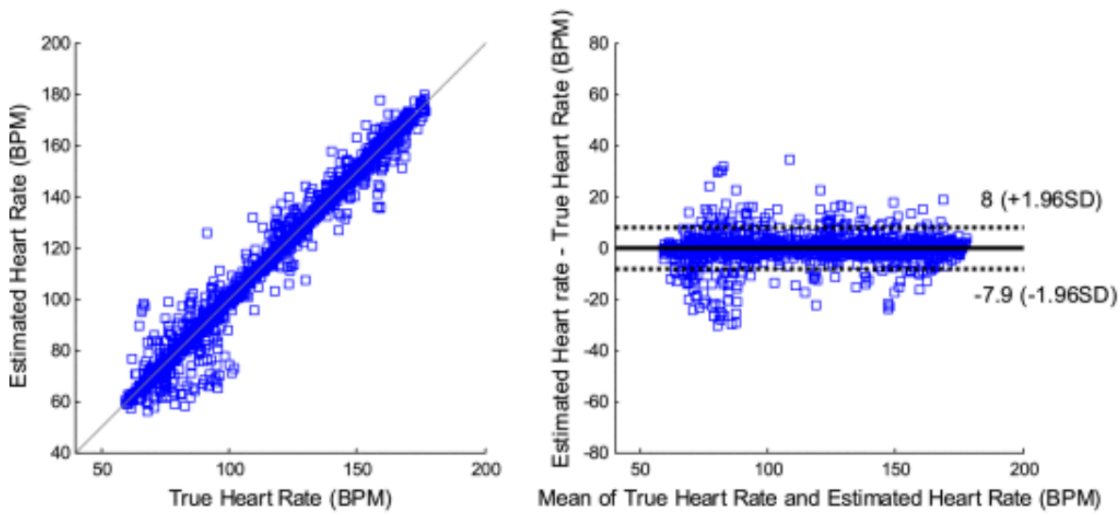

Figure 16: Predicted HR and error over ground truth HR for Temko’s algorithm on the TROIKA dataset. The mean and 95% confidence interval of the error is also shown [77].

Category	Name	MAE [BPM]	MAPE [%]
Spectrum-based	FFT Peaks [68]	1.084	1.435
Peak-based	BIOBSS Beats [69]	1.237	1.387
Threshold-based	HeartPy [73], [74]	0.466	0.506
Dummy	Random (50–150 BPM)	29.672	36.088

Table 7: Accuracy of the best performers on the 13 medium-quality CapnoBase recordings.

The accuracy of the best performers have also been tested on 13 additional recordings of the CapnoBase dataset which contain a few motion artefacts. The results are reported in Table 7, and they are much better than in Table 6, although slightly worse than in the ideal case. The importance of getting a clean-enough signal is therefore shown.

To further understand where this increased error rate on the TROIKA dataset comes from, the signals can be inspected. For both datasets, the occurrence of a motion artefact on the PPG signal is shown in Figure 17. They hint at a major difference: on the CapnoBase dataset, the signal is generally very clean and regular, and the motion artefacts are usually a brief loss of the signal. Moreover, they are very rare, there are only a handful (< 10) per recording of 8 minutes. In contrast, motion artefacts on the TROIKA dataset are much more present: the signal's amplitude can vary a lot, and there are additional tones mixed in the signal that distort it heavily. This is the case for most of the recording, and not only during specific moments. On this type of data, peak-based methods are understandably more prone to errors, and matching the frequency spectra of the PPG and acceleration signals isn't sufficient to identify the frequency of the heart beats. This is why state-of-the-art algorithms tend to use much more advanced methods on noisy data.

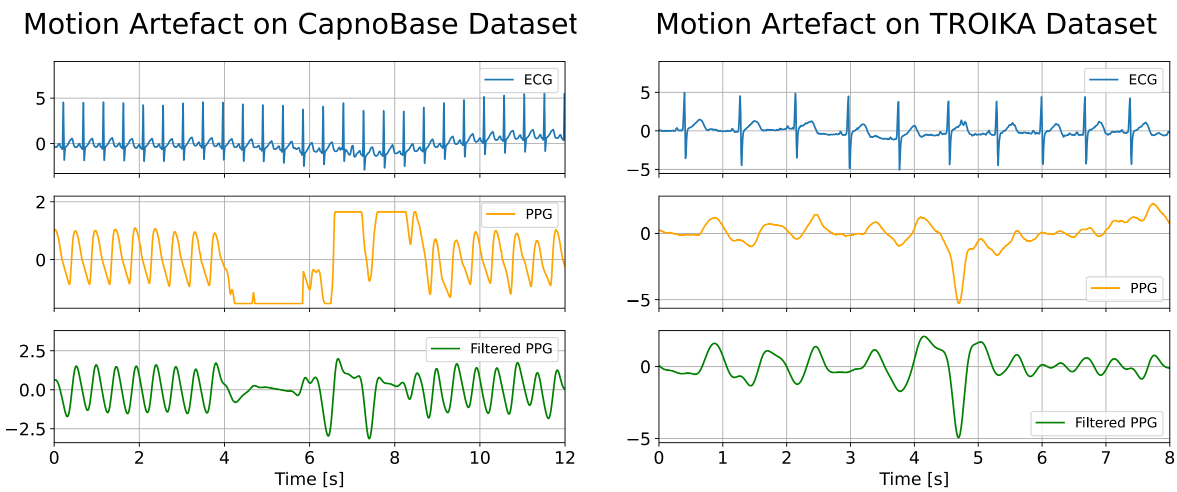

(a) On the CapnoBase dataset (noisier recordings). *(b) On the TROIKA dataset.*

Figure 17: Examples of motion artefacts affecting the PPG signal.

2.4. Chapter conclusion

In summary, several simple approaches have been identified to extract HR from a PPG signal. The results obtained on a clean signal are overall very good, but once motion artefacts are introduced, the accuracy drops significantly. This is a big problem for the targeted application. The algorithm that has been used for the prototype is a lightened version of HeartPy designed for Arduino micro-controllers, which can be found on van Gent's GitHub page [80]. It also uses a moving average for peak detection, but doesn't use a hyper-parameter to refine the selection. Instead, intervals between peaks are simply filtered by comparing them to the previous intervals, and to specified maximum and minimum HR values. The scaling of the signal is also done dynamically. This algorithm has the advantage of already being written in C, which made it the only option available due to a lack of time. For future work on this topic, it would be interesting to use or develop an algorithm with more advanced signal processing techniques, such as that of Temko [77]. It could also be interesting to exploit multiple PPG channels to enhance robustness. The TROIKA dataset comprises two channels, and many PPG sensors can emit at different wavelengths, typically infrared, red and green, which react in different ways with the skin. This has not been explored further in this work.

Chapter 3
Prototype Design

In this chapter, the algorithm selected in Chapter 2 is implemented and tested on a wearable sensor platform. It is powered via a USB cable, and senses the heart rate of the subject in contact with its sensor. It then sends this information to a connected device via a Bluetooth® Low Energy connection. A smartphone is used to receive the data, to simulate a part of the firefighting PPE that would relay it to the entry management system. First, the selection process for the hardware is explained, and the selected platform is presented. Then, the software implementation is detailed, from its architecture to the signal processing algorithm. Finally, the prototype's behaviour is tested, and improvements are suggested along the way.

3.1. Hardware selection

In this section, the process used for selecting a suitable hardware platform is detailed. The search for relevant solutions is aimed at sensor evaluation kits for their more advanced design (more compact, with more features, etc.) and the development time and effort they save, compared to an implementation using raw components on custom printed circuit boards (PCBs). Their drawbacks tend to be their increased price and the difficulty to customise them. The kits have been found on the main website of Analog Devices, by using the keyword "PPG" and, for each reported PPG-related product, listing the given evaluation kits/reference designs. The sites of other electronic component designers, such as Texas Instruments, have not been searched because of a lack of time and because satisfying solutions had already been found. Table 8 and Table 9 list and describe them. A unique ID number has been assigned to each of them to make the tables more concise: the entry number 1 in Table 8 concerns the same kit as the entry number 1 of Table 9, and so on.

Table 8 shows their names (with clickable links to their product pages), their prices as reported on Mouser, a description of what they are, their size, and an evaluation of whether their hardware and software can be customised. The latter is reported using the same colour code as before, with a green square (■) for "easy customisation", an orange diamond (◆) for "possible customisation", and a red circle (●) for "difficult customisation". For hardware, this is evaluated by judging whether it could be possible to add new components. Typically, the absence of communication pins or extra space into the system makes this rating worse. For software, it is evaluated by investigating whether the program of the main processor could be changed. Typically, providing only a pre-compiled firmware and a graphical user interface to stream the data and modify settings is not enough to get a good rating. This metric is important for the prototype to be modular, upgradable, and reusable for other projects. The sizes that were reported in orange have been estimated from pictures because they are not indicated in the documentation. Some information is under a non-disclosure agreement (or simply not given), which means it could not be reported in the table and is instead replaced with a question mark (?). For entries number 1, 13 and 14, a second product has to be bought separately to complete the kit. The price shown for entry 1 is that of both products. In the case of entry 13, the second product wasn't available as a separate product at the time of writing (only as part of a different evaluation kit), and for entry 14, there are no recommended MCUs, so the price depends on the chosen MCU.

ID	Name & Link	Price [€]	Description	Size [mm]	Customisation	
					HW	SW
1	MAX30101WING + MAX32630FTHR	69.14	2 PCBs	51x23	■	■
2	MAXM86161EVSYS	183.86	PCB + flex cable	28x15+53x6	◆	■
3	MAX86916EVSYS	210.11	2 PCBs	51x23	■	■
4	MAX86173EVSYS	200.6	Bracelet	40x18	●	◆
5	MAXREFDES101	485.45	Bracelet	40x25	●	■
6	MAX-HEALTH-BAND	220.62	Bracelet	40x18	●	■
7	MAXREFDES105	280.15	Bracelet	40x18	●	■
8	MAXREFDES220	593.47	2 PCBs	51x23	■	■
9	MAXREFDES103	261.95	Bracelet	40x18	●	■
10	MAX86140EVSYS	147.08	Bracelet	40x18	◆	●
11	MAXREFDES282	660.73	Chest patch	?	?	■
12	MAXREFDES104	490.26	Bracelet	40x18	●	■
13	EVAL-ADPD4100-4101 + EVAL-ADPDM3Z	>114.18	2 PCBs	25x25 +60x40	◆	●
14	MAXREFDES117 (+ separate MCU)	>18.06	PCB (+ MCU to buy separately)	13x13 + …	■	■

Table 8: Comparison of PPG evaluation boards: price, description, size and rated accessibility to customisation.

ID	Sensor	MCU	Battery	Extra features
1	MAX30101	MAX32630	No	USB, bat. charger
2	MAXM86161	MAX32664	LiPo 3.7V 105mAh	USB
3	MAX86916	MAX32630	No	USB, bat. charger
4	MAX86173	?	LiPo 3.7V 105mAh	USB, bat. charger
5	MAX86141	MAX32630	LiPo 3.7V 105mAh	USB, bat. charger, ECG/BioZ AFE, T° sensors, display
6	MAX86140	?	LiPo 3.7V 105mAh	bat. charger
7	MAX86174A	MAX32630	Yes	?
8	MAX30101	MAX32630	No	USB, bat. charger
9	MAX86141	MAX32630	Yes	USB, bat. charger
10	MAX86140	MAX32620	No	USB, bat. charger
11	MAX86178	ISP1807	LiPo 3.V 190mAh	USB, bat. charger, ECG/BioZ AFE, T° sensor
12	MAX86176	MAX32666	No	USB, bat. charger, ECG AFE, T° sensor
13	MAX86176	MAX32666	No	USB, bat. charger, ECG/BioZ AFE
14	MAX30102	N/A	No	N/A

Table 9: Comparison of PPG evaluation boards: sensor, micro-controller unit (MCU), provided battery and additional features.

Table 9 gives more information on the features of each kit, by showing the name of the raw PPG sensor and of the micro-controller unit (MCU), reporting whether a battery is provided, and listing the extra sensors and components built in. All kits also have a built-in Bluetooth® Low Energy (BLE) radio, and an accelerometer and/or gyroscope, except entry number 14 that requires a MCU to be bought separately.

The platform that has been chosen is entry number 1, the MAX30101WING and MAX32630FTHR combination, for its low price, acceptable size, hardware modularity and easy access to source code. Entries 8 and 14 have also been considered, but the former is a lot more expensive, and the latter would have required time to look for a MCU and to create a system that connects them together. After some reconfiguration of the pin headers, the resulting prototype is shown in Figure 18. The output can be read on a smartphone using the nRF Connect application for Android phones.

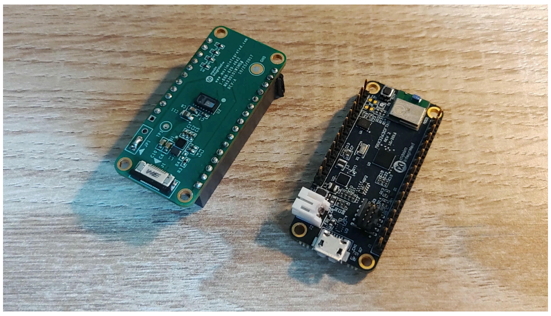

(a) The sensor evaluation board (left), and the micro-controller unit (right).

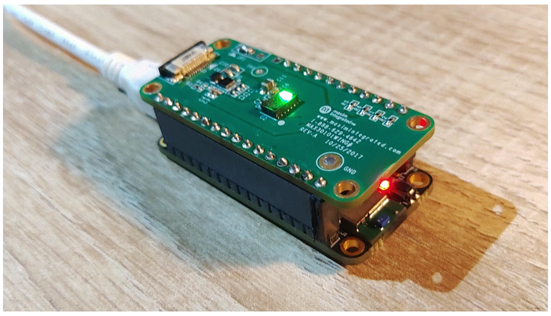

(b) Both assembled together and powered.

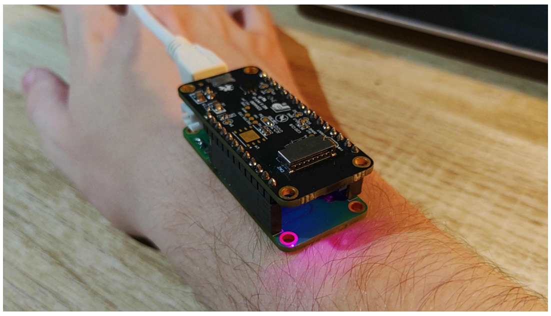

(c) On the skin of a subject.

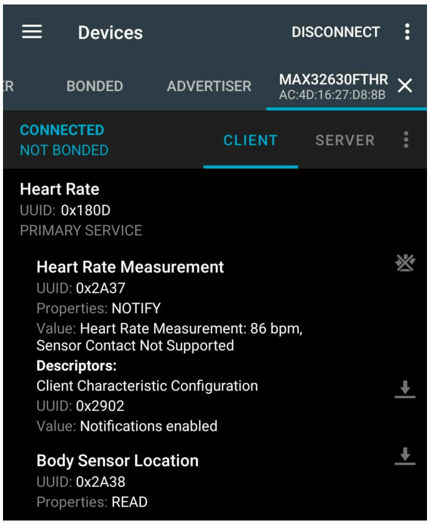

(d) Smartphone interface.

Figure 18: The prototype composed of the MAX30101WING and MAX32630FTHR, as well as the smartphone interface (nRF Connect for Android).

3.2. Software implementation

The software is inspired from open-source example codes for the MAX32630FTHR MCU. It works with an event queue, which puts the processor to sleep and wakes it periodically to complete tasks in "first in, first out" order. There are three different types of tasks:

- Retrieving and storing samples from the MAX30101 PPG sensor using the I²C communication bus, which is done every 180 milliseconds. These samples are taken by the sensor at a rate of 100 Hz.
- Track the HR of the user by analysing the collected samples and send the result through the BLE radio (if a receiver is connected), which is done every 1.8 seconds.
- Handle the BLE radio events, such as connections, disconnections, queries, etc., which is done when required.

This architecture allows to reduce the power consumption a bit compared to one that uses an infinite loop to cycle between tasks. Power consumption is further addressed in Section 3.3.2. The behaviour of the sensor on the BLE network is to simply advertise itself as a HR-tracking wearable sensor when it isn't paired with another device, and send the estimated HR value when it is asked by a paired device. This is done with BLE's generic access profile and generic attribute profile.

The signal processing algorithm, which initially was the MAX30101WING example code that has been tested in Chapter 2 and has showed mediocre results, has been replaced with a more reliable and maintainable alternative. First, the low-pass finite-impulse-response filter with a 5Hz cutoff frequency has been replaced with a second order band-pass Butterworth infinite-impulse-response filter, the pass-band of which stands between 0.75 Hz (45 BPM) and 3.33 Hz (200 BPM). The coefficients of a first order band-pass Butterworth have been computed using SciPy's `butter` function. To double the order, the first order filter is simply applied twice. Unfortunately, a filter of higher order could not be achieved because of an instability problem that could not be solved in time. The frequency response of the filter is shown in Figure 19. For a digital filter, it is not very sharp because of its low order. This means the pass-band is not very flat, but tests have shown that this is not a problem since the band of interest is not very large either, so it is preferable to cut anything outside of it and let the HR tracking algorithm scale the signal of interest.

Figure 20 shows a raw PPG recording and the resulting signal after applying the filter. The signals have been shifted vertically to be able to zoom in on them, since the raw signal has a DC component of 25000 units. The baseline of the raw signal (the component below 0.75 Hz) can be affected by different effects, which can disturb peak-detection based tracking. Between the 25th and 35th second, an artefact has been intentionally added by pressing the sensor firmly on the skin of the subject. The filter successfully removes the significant baseline changes, the artefact and the high frequency noise, while keeping the signal of interest intact. During the artefact, the filtered signal greatly reduces in amplitude, likely because pressing the sensor too hard on the skin blocks some of the blood flow under it.

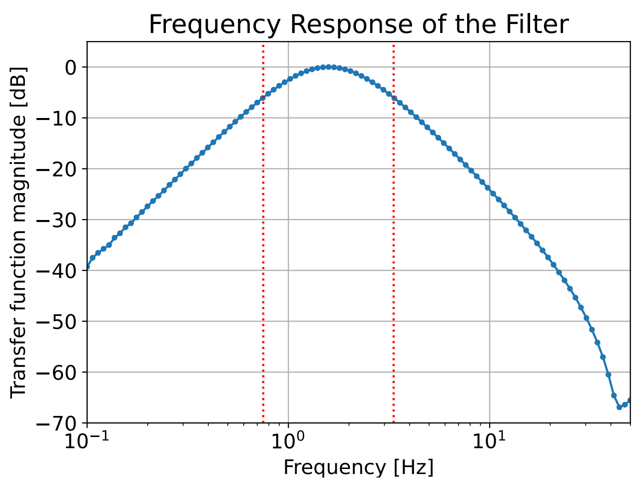

Figure 19: Frequency response of the digital filter. Cutoff frequencies are shown in red.

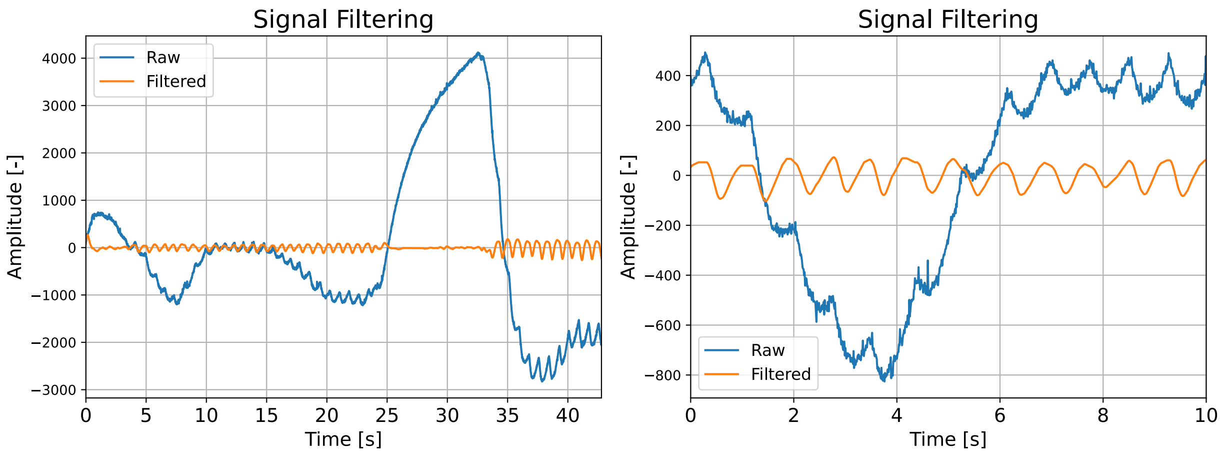

(a) On low-frequency noise and artefacts. *(b) On high frequency noise.*

Figure 20: Effect of the filter on a raw PPG signal.

The samples are then processed using a lightened version of HeartPy intended for Arduino micro-controllers, provided by van Gent [80]. This version also uses a moving average for peak detection, but it doesn't use a hyper-parameter to optimise the threshold. It does have a way of estimating the local range of the signal, however. HR is computed using the mean of the intervals between recent peaks. The tracking is done using only one LED, so the green LED has been chosen because green is preferred for HR tracking (while red and infrared usually are used to compute the oxygen saturation of blood). This algorithm has been chosen because it is already implemented in C++, which saved time.

The software has been implemented in C++ with the ARM Mbed operating system version 5.9.7. It has been developed and compiled using ARM's Keil Studio Cloud environment. The latest version of Mbed, 6.17.0, could not be used because there seem to be incompatibilities with the MAX32630FTHR MCU. Version 5.10 or higher doesn't support the usage of the USB port, while versions 6 doesn't support the Bluetooth® radio. Version 5.9.7 is the latest that allows to use both. According to unofficial sources on the Mbed forum, this is because the platform software hasn't been maintained properly by Maxim Integrated. In any case, ARM have announced in August 2024 that Mbed is reaching end of life in July 2026, meaning its websites will be archived and the software will no longer receive any updates, although the latter will still be open-source and publicly available. ARM is recommending to either use the community editions of Keil Studio and Mbed, or to move away from Mbed and turn towards alternative operating systems. Arduino, a very popular operating system, seems to support the MAX32630FTHR board, although example codes are more rare than on Mbed. Other operating systems such as FreeRTOS and Zephyr don't support this board, but they can be adapted to boards with an ARM Cortex-M4 processor such as this one. Alternatively, a different MCU could replace the MAX32630FTHR. Many designers on the market propose similar products, e.g., STMicroelectronics, Arduino or Silicon Labs.

3.3. Characterisation of the prototype

3.3.1. Functional assessment

To confirm that the prototype works correctly, it's internal outputs are shown on Figure 21. The raw PPG signal and the filtered signal show how the filter removes baseline changes and high-frequency noise. Peaks are then identified on the filtered signal. The true peaks (light-green circles) have been located using SciPy's `find_peaks` function in post-processing. The peaks detected by the algorithm in real time are marked with crosses. The green ones fit the expectations and are thus used for the computation of the HR, while the red ones are rejected, meaning the interval between it and the previous peak is ignored for the computation. This is because they are either too close or too far to the previous one.

Three different experiments have been made. In the first experiment (Figure 21(a)), the subject isn't moving. The majority of peaks are correctly identified, and the algorithm quickly recovers when it misses one. The predicted HR throughout the window is around 95–101 BPM, which corresponds to what is observed on the raw signal. In the second

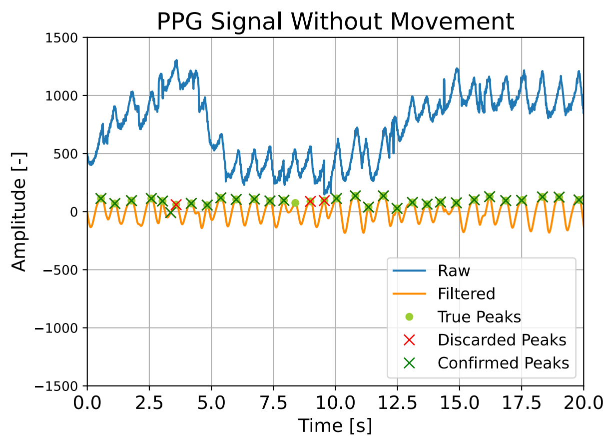

(a) When the subject doesn't move.

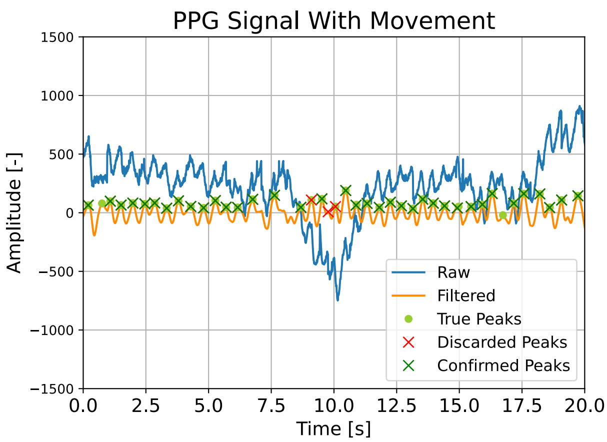

(b) When the subject is moving.

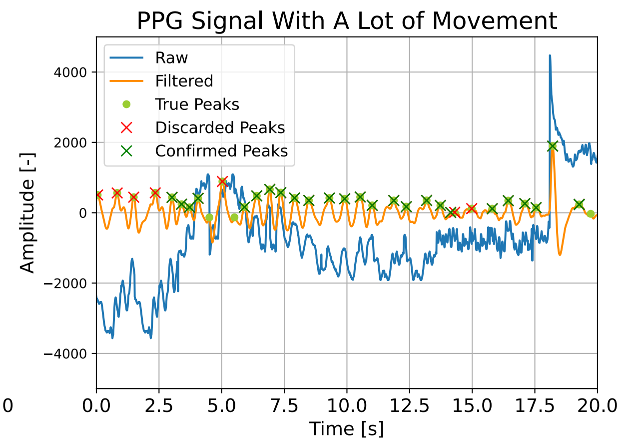

(c) When artefacts are intentionally created.

Figure 21: Algorithm output on data captured and analysed in real time.

experiment (Figure 21(b)), the subject is running in place, which creates some artefacts and increases the HR. The predicted HR is around 114–127 BPM, which is a bit low compared to the 44 beats of the raw signal in the 20 second window. This is because the algorithm has missed a few peaks. In the third experiment (Figure 21(c)), the subject stands still and motion artefacts are intentionally created by irregularly pushing the sensor around on the skin (while still maintaining contact). In that case, both the raw and filtered signals are hard to manually interpret. This experiment shows why further tests on robustness would require a system to derive a reference HR, so that the error metrics of the prototype could be measured.

3.3.2. Power consumption and battery

It has been estimated that the prototype consumes 45.51 mW of power under normal operations, 33.30 mW when gathering and analysing samples but not using the radio, and 19.24 mW when putting the processor to sleep at all times (thus leaving only the power consumption of the sensor, of the other components and the sleep power of the processor). The hypothesis can then be made that the power consumed at the battery is spread somewhat evenly between handling samples, using the radio, and powering the other components on the board (power management chips, peripherals, sensors, etc.). As it stands, this is likely acceptable, since it would mean the prototype would last 8.5h using one of the Li Po 3.7V 105mAh battery proposed in some of the evaluation kits of Section 3.1. Firefighter interventions usually don't last this long. Still, this is a design aspect that should arguably be optimised for any electronic system, for the sake of eco- and consumer-friendliness. Not all possibilities have been explored to optimise the tradeoff between PPG signal amplitude, frequency of the HR tracking updates and power consumption. There are many choices to consider for that matter: active PPG LEDs (red, infrared and/or green), LED current and pulse width, sampling rate, sample averaging, radio transmitter power, BLE advertising intervals, the use of power save modes on the sensor, the processor, the radio and other peripherals, etc. In addition, designers should be wary of fire hazards caused by batteries, especially in the context of firefighting. The battery technology and casing should be chosen accordingly, such that it can resist high temperatures and resist mechanical constraints.

3.3.3. Ease of use

In the context of firefighting, it would be an inconvenience to have to manually setup the connection between the sensor and the rest of the equipment, similarly to how the prototype is used. Moreover, if firefighters begin using wireless sensors of this kind, the equipment has to be linked to the sensor of its user, and not of another firefighter. Ideally, the two should connect to each other automatically by having each unpaired sensor advertise with a unique identifier and the equipment to look for the identifier that corresponds to its user. Additionally, this would make the reconnection automatic in case of a disconnection. For that matter, two solutions have been imagined:

- Link the sensor and the equipment before the intervention by saving the identifier of the sensor into the equipment's software. This means that each set of equipment is paired to its unique sensor, and that they should not be mixed with the others.
- Be able to link the two quickly enough at the start of the intervention by bringing the two in close proximity to exchange identifiers. For example, the equipment could be capable of reading a simple RFID tag on the sensor that contains the necessary information, typically the identifier the sensor advertises when its unpaired.

3.4. Chapter conclusion

In summary, this chapter showed the complete design of the prototype that has been used as a proof of concept for this work. The platform chosen can rather easily be customised in terms of hardware and software, and already comprises all that is required for this work: a digital PPG sensor, a micro-controller, a radio, an accelerometer, a battery port and some debugging features such as a USB port and LEDs. The example code that came with the kit has been greatly upgraded, both in terms of features (namely, BLE communication) and in terms of reliability. The low-pass filter has been replaced by a band-pass filter that greatly increases the signal's quality, and the HR tracking algorithm is now easily maintainable. It is also much more robust, since it can scale the signal dynamically, adapt its threshold, and reject outliers from its average. Unfortunately, an embedded version of the best performers of Chapter 2 could not have been implemented to track HR due to a lack of time, and the digital filter could also receive some improvements. The accelerometer data also hasn't been exploited to possibly compensate motion artefacts. Finally, many more aspects have to be addressed when continuing the development of this project, from optimising power consumption and signal amplitude, to choosing a resistant battery, to conveniently integrating the system into actual firefighter PPE. The prototype could also be improved by using customised boards with more advanced hardware (e.g., a sensor hub to lower power consumption) and the Mbed operating system could be replaced by one that will keep receiving updates and support.

Conclusion

Monitoring vital signs of firefighters in intervention is a field that is still emerging, with new products likely to arrive on the market soon. Personal protective equipment for firefighting already benefits in many ways from the advancements in radio communication and the miniaturisation of sensors and electronics. It allows firefighters to remotely communicate with their teammates, see in low visibility conditions, and call for help automatically in emergency situations. Vital signs monitoring is likely one of the next features to be added. The interest comes from the fact that many firefighters suffer and/or die from cardiovascular diseases caused by frequent exposure to high stress levels, both psychologically and physiologically. There are many variables that inform on the firefighter's condition and fitness, including heart rate, breathing rate, hydration, body temperature and body movements. Each of these variables can be measured with several techniques that have been presented, but many require more research to be done before they can be used in the context of firefighting. Given the context of this work, heart rate was chosen to be the main focus because it is highly correlated with psychophysiological stress and rather easy to sense.

To sense it, photoplethysmography is a simple and non invasive technique, where a light is emitted on the skin, and the amount of light that reflects back depends on the body's composition. When blood pulses, more or less light is absorbed, thus changing the intensity of the light received. These sensors are easy to find on the market, but can be tricky to master because of their sensitivity to artefacts caused by the user's movement. Three different approaches were compared to derive the heart rate from the signal: spectrum-based, peak-based and threshold-based algorithms. These three categories were compared in terms of mean absolute error thanks to two separate datasets: one without (or with few) motion artefacts, and one with many. All three have a comparable performance that is excellent when a mid- to high-quality signal is given, but having too many motion artefacts can greatly worsen that performance beyond what is acceptable. Spectrum-based algorithms tend to perform better because they can use the signal of an accelerometer to compensate for some of the motion artefacts, but the performance of the one that was tested was still unacceptable. It is recommended to turn towards the scientific literature to find more advanced signal processing techniques, such as signal decomposition and adaptative filtering for example. In fact, many articles detail more or less how to achieve excellent results even when the signal is heavily affected, and some provide access to an open-source implementation.

Finally, a prototype was built and qualitatively tested as a proof of concept. It is composed of two evaluation boards: one with the sensor and the other with the micro-controller. The sensor stores samples that it takes at a rate of 100 Hz, and they are periodically retrieved by the micro-controller. The micro-controller applies a band-pass filter to remove high-frequency noise and baseline changes. It then tracks the heart rate using a robust threshold-based algorithm. Unfortunately, a more advanced algorithm could not be implemented in time. The prototype can then send the estimated heart rate to a paired device connected via Bluetooth® Low Energy. There are many aspects that could be improved regarding the prototype. First, the filter could be made with a higher order to flatten the pass-band, while still cutting as much noise outside the band as possible. Second, the heart rate tracking could be made with an algorithm that is more robust to motion artefacts, especially if they are in the same frequency band as the heart rate. The performance of the whole system could be verified with a separate system that derives a reference heart rate. In addition, many settings could be tuned to lower power consumption while retaining a good signal amplitude. It is also recommended to find an alternative operating system to replace the one currently in use, since it will soon reach end of life. Finally, to successfully integrate the system into the firefighter's equipment, the battery must be chosen such that it is resistant to shocks and high temperature, and the wireless connection between the devices should be established with as few inputs from the user as possible.

In summary, there are many relevant aspects still to be addressed on the topic of vital signs monitoring for firefighters, regarding the design of the prototype, its software implementation, its heart rate tracking, but also regarding other techniques and other variables of interest.

Bibliography

[1] J. Taborri, S. Pasinetti, L. Cardinali, F. Perroni, and S. Rossi, ‘Preventing and Monitoring Work-Related Diseases in Firefighters: A Literature Review on Sensor-Based Systems and Future Perspectives in Robotic Devices’, *International Journal of Environmental Research and Public Health*, vol. 18, no. 18, 2021, doi: 10.3390/ijerph18189723.

[2] S. Rodrigues, D. Dias, J. S. Paiva, and J. P. Cunha, ‘Psychophysiological Stress Assessment Among On-Duty Firefighters’, in *2018 40th Annual International Conference of the IEEE Engineering in Medicine and Biology Society (EMBC)*, 2018, pp. 4335–4338. doi: 10.1109/EMBC.2018.8513250.

[3] M. A. Cvirn *et al.*, ‘The effects of hydration on cognitive performance during a simulated wildfire suppression shift in temperate and hot conditions’, *Applied Ergonomics*, vol. 77, pp. 9–15, 2019, doi: https://doi.org/10.1016/j.apergo.2018.12.018.

[4] R. F. Fahy, J. T. Petrillo, and J. L. Molis, ‘Firefighter Fatalities in the US – 2019.’, 2020, [Online]. Available: http://tkolb.net/FireReports/2020/FF_FatalitiesUS2019.pdf

[5] A. Wolkow *et al.*, ‘Coronary Heart Disease Risk in Volunteer Firefighters in Victoria, Australia’, *Archives of Environmental & Occupational Health*, vol. 69, no. 2, pp. 112–120, 2014, doi: 10.1080/19338244.2012.750588.

[6] E. S. Soteriades, D. L. Smith, A. J. Tsismenakis, D. M. Baur, and S. N. Kales, ‘Cardiovascular Disease in US Firefighters: A Systematic Review’, *Cardiology in Review*, vol. 19, no. 4, 2011, doi: 10.1097/CRD.0b013e318215c105.

[7] R. Fahy, B. Evarts, and G. P. Stein, ‘U.S. fire department profile’, 2022, [Online]. Available: https://www.nfpa.org/education-and-research/research/nfpa-research/fire-statistical-reports/us-fire-department-profile

[8] RTL Info and Belga, ‘Maxime, pompier décédé dans l'incendie de la prison de Lantin, a été prisonnier d'un "effet four": qu'est-ce précisément?’, *RTL Info*, May 2025, Accessed: Jun. 24, 2025. [Online]. Available: https://www.rtl.be/actu/belgique/faits-divers/maxime-pompier-decede-dans-lincendie-de-la-prison-de-lantin-ete-prisonnier-dun/2025-05-30/article/751615

[9] RTBF Actus and Belga, ‘Des hommages publics seront rendus au pompier décédé dans l'incendie de l'hôtel Sheraton’, *RTBF Actus*, Mar. 2022, Accessed: Jun. 24, 2025. [Online]. Available: https://www.rtbf.be/article/des-hommages-publics-seront-rendus-au-pompier-decede-dans-l-incendie-de-l-hotel-sheraton-10961432

[10] RTBF Actus and Belga, ‘Bruxelles : un pompier décède pendant une intervention sur un incendie à l’hôtel Sheraton, place Rogier’, *RTBF Actus*, Mar. 2022, Accessed: Jun. 24, 2025. [Online]. Available: https://www.rtbf.be/article/bruxelles-un-pompier-decede-pendant-une-intervention-sur-un-incendie-a-l-hotel-sheraton-place-rogier-10955925

[11] P. Wagner, B. Messerschmidt, S. Sokolov, and H. Herweg, ‘World Fire Statistics’, 2024, [Online]. Available: https://www.ctif.org/commissions-and-groups/ctif-center-world-fire-statistics

[12] Drägerwerk AG & Co., ‘Dräger PSS® AirBoss’, 2025, [Online]. Available: https://www.draeger.com/fr_be/Products/PSS-AirBoss

[13] C. Grant, A. Jones, A. Hamins, and N. Bryner, ‘Realizing the Vision of Smart Fire Fighting’, *National Institute of Standards and Technology Special Publication*, no. 1191, 2015, doi: 10.6028/NIST.SP.1191.

[14] X. Chai, R. Wu, M. Pike, H. Jin, W.-Y. Chung, and B.-G. Lee, ‘Smart Wearables with Sensor Fusion for Fall Detection in Firefighting’, *Sensors*, vol. 21, no. 20, 2021, doi: 10.3390/s21206770.

[15] L. T. Nascimento *et al.*, ‘A Smart Wearable System for Firefighters for Monitoring Gas Sensors and Vital Signals’, in *XXVII Brazilian Congress on Biomedical Engineering*, T. F. Bastos-Filho, E. M. de Oliveira Caldeira, and A. Frizera-Neto, Eds., Cham: Springer International Publishing, 2022, pp. 1333–1340. doi: https://doi.org/10.1007/978-3-030-70601-2_198.

[16] G. Song, S. Mandal, and R. M. Rossi, Eds., ‘1 - Introduction’, *Thermal Protective Clothing for Firefighters*. in Woodhead Publishing Series in Textiles. Woodhead Publishing, pp. 1–4, 2017. doi: https://doi.org/10.1016/B978-0-08-101285-7.00001-0.

[17] Sioen Firefighter Clothing, ‘Belgium’, 2025, [Online]. Available: https://sioenfire.com/en/fire-fighter-suits/8vj1a2pvt

[18] Viking Life Saving Equipment A/S, ‘VIKING Firefighter Hood with DuPont™ Nomex® Nano Flex Technology - Light Grey’, 2025, [Online]. Available: https://www.viking-fire.com/en/products/viking-fire-hoods/viking-fire-hood-partx/ps384168/

[19] MSA Safety Inc., ‘Gallet F1 XF and Accessories’, 2025, [Online]. Available: https://fr.msasafety.com/Fire-Helmets/Fire-Helmets/Gallet-F1-XF-and-Accessories/p/000360008000001001

[20] Drägerwerk AG & Co., ‘Dräger FPS®-COM 5000’, 2025, [Online]. Available: https://www.draeger.com/fr_be/Products/FPSCom5000

[21] MSA Safety Inc., ‘C1 Communication Module for G1 Mask’, 2025, [Online]. Available: https://nl.msasafety.com/Supplied-Air-Respirators-%28SCBA%29/Communication-Systems/C1-Communication-Module-for-G1-Mask/p/0000100009000W1000

[22] ASTRID, ‘ASTRID de A à Z’, 2023, [Online]. Available: https://www.astrid.be/sites/public/files/2023-04/AST-104_Brochure%20van%20AtotZ_FR_lowres.pdf

[23] H. A. Snapp, N. Schaefer Solle, B. Millet, and S. M. Rajguru, ‘Subclinical Hearing Deficits in Noise-Exposed Firefighters’, *International Journal of Environmental Research and Public Health*, vol. 19, no. 17, 2022, doi: 10.3390/ijerph191711028.

[24] K. S. Root, C. Schwennker, D. Autenrieth, D. R. Sandfort, T. Lipsey, and W. J. Brazile, ‘Firefighter Noise Exposure During Training Activities and General Equipment Use’, *Journal of Occupational and Environmental Hygiene*, vol. 10, no. 3, pp. 116–121, 2013, doi: 10.1080/15459624.2012.753023.

[25] O. Hong, D. Samo, R. Hulea, and B. Eakin, ‘Perception and Attitudes of Firefighters on Noise Exposure and Hearing Loss’, *Journal of Occupational and Environmental Hygiene*, vol. 5, no. 3, pp. 210–215, 2008, doi: 10.1080/15459620701880659.

[26] Firecom, ‘FHW507.V2’, 2025, [Online]. Available: https://www.firecom.com/products/wireless-headsets/fhw507/

[27] MSA Safety Inc., ‘Connected Firefighter’, 2025, [Online]. Available: https://nl.msasafety.com/connected-firefighter

[28] Drägerwerk AG & Co., ‘Dräger FireGround’, 2025, [Online]. Available: https://www.draeger.com/fr_be/Products/FireGround

[29] Drägerwerk AG & Co., ‘Dräger UCF® FireVista’, 2025, [Online]. Available: https://www.draeger.com/fr_be/Products/UCF-FireVista

[30] MSA Safety Inc., ‘MSA LUNAR’, 2025, [Online]. Available: https://nl.msasafety.com/Connected-Firefighter/LUNAR/LUNAR/p/000010002400001000

[31] Drägerwerk AG & Co., ‘Dräger UCF® FireCore : la vision infra-rouge intégrée au masque’, 2025, [Online]. Available: https://www.draeger.com/fr_be/Safety/UCF-FireCore

[32] Qwake Technologies, ‘C-THRU’, 2025, [Online]. Available: https://www.qwake.tech/

[33] Y. Chong *et al.*, ‘Cooperative Localization of Firefighters Based on Relative Ranging Constraints of UWB and Autonomous Navigation’, *Electronics*, vol. 12, no. 5, 2023, doi: 10.3390/electronics12051181.

[34] D. D. Arumugam, P. Littlewood, N. Peng, and D. Mishra, ‘Long-Range Through-the-Wall Magnetoquasistatic Coupling and Application to Indoor Position Sensing’, *IEEE Antennas and Wireless Propagation Letters*, vol. 19, no. 3, pp. 507–511, 2020, doi: 10.1109/LAWP.2020.2967069.

[35] R. Dekimpe and D. Bol, ‘ECG Arrhythmia Classification on an Ultra-Low-Power Microcontroller’, *IEEE Transactions on Biomedical Circuits and Systems*, vol. 16, no. 3, pp. 456–466, 2022, doi: 10.1109/TBCAS.2022.3182159.

[36] A. Nicolò, C. Massaroni, and L. Passfield, ‘Respiratory Frequency during Exercise: The Neglected Physiological Measure’, *Frontiers in Physiology*, vol. 8, 2017, doi: 10.3389/fphys.2017.00922.

[37] T. Hussain, S. Ullah, R. Fernández-García, and I. Gil, ‘Wearable Sensors for Respiration Monitoring: A Review’, *Sensors*, vol. 23, no. 17, 2023, doi: 10.3390/s23177518.

[38] A. M. Holland-Winkler and B. K. Hamil, ‘Hydration Considerations to Improve the Physical Performance and Health of Firefighters’, *Journal of Functional Morphology and Kinesiology*, vol. 9, no. 4, 2024, doi: 10.3390/jfmk9040182.

[39] I. S. Gavin P. Horn Jacob DeBlois and D. L. Smith, ‘Quantifying Dehydration in the Fire Service Using Field Methods and Novel Devices’, *Prehospital Emergency Care*, vol. 16, no. 3, pp. 347–355, 2012, doi: 10.3109/10903127.2012.664243.

[40] D. T. Gottuk, M. J. Peatross, J. P. Farley, and F. W. Williams, ‘The development and mitigation of backdraft: a real-scale shipboard study’, *Fire Safety Journal*, vol. 33, no. 4, pp. 261–282, 1999, doi: https://doi.org/10.1016/S0379-7112(99)00033-8.

[41] T. Graham, G. Makhviladze, and J. Roberts, ‘On the theory of flashover development’, *Fire Safety Journal*, vol. 25, no. 3, pp. 229–259, 1995, doi: https://doi.org/10.1016/0379-7112(95)00049-6.

[42] M. Del Sal, E. Barbieri, P. Garbati, D. Sisti, M. B. L. Rocchi, and V. Stocchi, ‘Physiologic Responses of Firefighter Recruits During a Supervised Live-Fire Work Performance Test’, *Journal of Strength & Conditioning Research*, vol. 23, no. 8, pp. 2396–2404, 2009, doi: 10.1519/JSC.0b013e3181bb72c0.

[43] J. S. Cuddy, J. A. Sol, W. S. Hailes, and B. C. Ruby, ‘Work Patterns Dictate Energy Demands and Thermal Strain During Wildland Firefighting’, *Wilderness*

& Environmental Medicine, vol. 26, no. 2, pp. 221–226, 2015, doi: 10.1016/j.wem.2014.12.010.

[44] F. Camera *et al.*, 'Monitoring of temperature stress during firefighters training by means of RFID epidermal sensors', in *2019 IEEE International Conference on RFID Technology and Applications (RFID-TA)*, 2019, pp. 499–504. doi: 10.1109/RFID-TA.2019.8892269.

[45] C. Davide *et al.*, 'Smart Garments for Emergency Operators: The ProeTEX Project', *IEEE Transactions on Information Technology in Biomedicine*, vol. 14, pp. 694–701, 2010, doi: 10.1109/TITB.2010.2045003.

[46] S. El Dimassi, J. Gautier, V. Zalc, S. Boudaoud, and D. Istrate, 'Body Water Volume Estimation Using Bio Impedance Analysis: Where Are We?', *IRBM*, vol. 45, no. 3, p. 100839, 2024, doi: https://doi.org/10.1016/j.irbm.2024.100839.

[47] S. Ramasamy and A. Balan, 'Wearable sensors for ECG measurement: a review', *Sensor Review*, vol. 38, no. 4, pp. 412–419, 2018, doi: 10.1108/SR-06-2017-0110.

[48] I. Wicaksono *et al.*, 'A tailored, electronic textile conformable suit for large-scale spatiotemporal physiological sensing in vivo', *npj Flexible Electronics*, vol. 4, no. 1, p. 5, Apr. 2020, doi: 10.1038/s41528-020-0068-y.

[49] C.-L. Shen *et al.*, 'Respiratory Rate Estimation by Using ECG, Impedance, and Motion Sensing in Smart Clothing', *Journal of Medical and Biological Engineering*, vol. 37, no. 6, pp. 826–842, Dec. 2017, doi: 10.1007/s40846-017-0247-z.

[50] F. Gao *et al.*, 'Wearable and flexible electrochemical sensors for sweat analysis: a review', *Microsystems & Nanoengineering*, vol. 9, no. 1, p. 1, Jan. 2023, doi: 10.1038/s41378-022-00443-6.

[51] G. Anania *et al.*, 'Development of a novel algorithm for human fall detection using wearable sensors', in *SENSORS, 2008 IEEE*, 2008, pp. 1336–1339. doi: 10.1109/ICSENS.2008.4716692.

[52] V. T. Pham, Q. B. Le, D. A. Nguyen, N. D. Dang, H. T. Huynh, and D. T. Tran, 'Multi-Sensor Data Fusion in A Real-Time Support System for On-Duty Firefighters', *Sensors*, vol. 19, no. 21, 2019, doi: 10.3390/s19214746.

[53] D. T. Weiler, S. O. Villajuan, L. Edkins, S. Cleary, and J. J. Saleem, 'Wearable Heart Rate Monitor Technology Accuracy in Research: A Comparative Study Between PPG and ECG Technology', *Proceedings of the Human Factors and Ergonomics Society Annual Meeting*, vol. 61, no. 1, pp. 1292–1296, 2017, doi: 10.1177/1541931213601804.

[54] A. Taebi, B. E. Solar, A. J. Bomar, R. H. Sandler, and H. A. Mansy, 'Recent Advances in Seismocardiography', *Vibration*, vol. 2, no. 1, pp. 64–86, 2019, doi: 10.3390/vibration2010005.

[55] Y. D'Mello *et al.*, 'Real-Time Cardiac Beat Detection and Heart Rate Monitoring from Combined Seismocardiography and Gyrocardiography', *Sensors*, vol. 19, no. 16, 2019, [Online]. Available: https://www.mdpi.com/1424-8220/19/16/3472

[56] M. Jafari Tadi *et al.*, 'A real-time approach for heart rate monitoring using a Hilbert transform in seismocardiograms', *Physiological Measurement*, vol. 37, no. 11, p. 1885, Sep. 2016, doi: 10.1088/0967-3334/37/11/1885.

[57] D. Lo Presti, F. Santucci, C. Massaroni, D. Formica, R. Setola, and E. Schena, 'A multi-point heart rate monitoring using a soft wearable system based on fiber optic technology', *Scientific Reports*, vol. 11, no. 1, p. 21162, Oct. 2021, doi: 10.1038/s41598-021-00574-2.

[58] B. Semiz *et al.*, 'Non-Invasive Wearable Patch Utilizing Seismocardiography for Peri-Operative Use in Surgical Patients', *IEEE Journal of Biomedical and Health Informatics*, vol. 25, no. 5, pp. 1572–1582, 2021, doi: 10.1109/JBHI.2020.3032938.

[59] P. S. Addison, J. N. Watson, M. L. Mestek, J. P. Ochs, A. A. Uribe, and S. D. Bergese, 'Pulse oximetry-derived respiratory rate in general care floor patients', *Journal of Clinical Monitoring and Computing*, vol. 29, no. 1, pp. 113–120, Feb. 2015, doi: 10.1007/s10877-014-9575-5.

[60] D. Blanco-Almazán, W. Groenendaal, F. Catthoor, and R. Jané, 'Wearable Bioimpedance Measurement for Respiratory Monitoring During Inspiratory Loading', *IEEE Access*, vol. 7, no. , pp. 89487–89496, 2019, doi: 10.1109/ACCESS.2019.2926841.

[61] C. Qiu, F. Wu, W. Han, and M. R. Yuce, 'A Wearable Bioimpedance Chest Patch for Real-Time Ambulatory Respiratory Monitoring', *IEEE Transactions on Biomedical Engineering*, vol. 69, no. 9, pp. 2970–2981, 2022, doi: 10.1109/TBME.2022.3158544.

[62] P. Aqueveque *et al.*, 'Simple Wireless Impedance Pneumography System for Unobtrusive Sensing of Respiration', *Sensors*, vol. 20, no. 18, 2020, [Online]. Available: https://www.mdpi.com/1424-8220/20/18/5228

[63] A. Fusco, D. Locatelli, F. Onorati, G. C. Durelli, and M. D. Santambrogio, 'On how to extract breathing rate from PPG signal using wearable devices', in *2015 IEEE Biomedical Circuits and Systems Conference (BioCAS)*, 2015, pp. 1–4. doi: 10.1109/BioCAS.2015.7348369.

[64] F. M. Williams-Bell, G. Boisseau, J. McGill, A. Kostiuk, and R. L. Hughson, 'Physiological responses and air consumption during simulated firefighting tasks in a subway system', *Applied Physiology, Nutrition, and Metabolism*, vol. 35, no. 5, pp. 671–678, 2010, doi: 10.1139/H10-061.

[65] R. M. Kesler, E. T. Hsiao-Wecksler, R. W. Motl, R. E. Klaren, I. Ensari, and G. P. Horn, ‘A modified SCBA facepiece for accurate metabolic data collection from firefighters’, *Ergonomics*, vol. 58, no. 1, pp. 148–159, 2015, doi: 10.1080/00140139.2014.964783.

[66] J. Park, H. S. Seok, S.-S. Kim, and H. Shin, ‘Photoplethysmogram Analysis and Applications: An Integrative Review’, *Frontiers in Physiology*, 2022, doi: 10.3389/fphys.2021.808451.

[67] T. Tamura, Y. Maeda, M. Sekine, and M. Yoshida, ‘Wearable Photoplethysmographic Sensors—Past and Present’, *Electronics*, vol. 3, no. 2, pp. 282–302, 2014, doi: 10.3390/electronics3020282.

[68] K. Strand, ‘Pulse_Rate_Estimation’, 2020, [Online]. Available: https://github.com/KJStrand/Pulse_Rate_Estimation

[69] Ç. Taşcı, İ. Karakuş, D. Çavuşoğlu, and F. Ç. Akyön, ‘BIOBSS’, 2023, [Online]. Available: https://github.com/obss/BIOBSS/tree/main

[70] J. Greene, ‘MAX30101WING_HR_SPO2’, 2018, [Online]. Available: https://os.mbed.com/teams/Maxim-Integrated/code/MAX30101WING_HR_SPO2/

[71] M. Tsai, ‘Sensor_PPG_MAX30102’, 2020, [Online]. Available: https://github.com/Mic-Tsai/Sensor_PPG_MAX30102

[72] M. Tsai, ‘Sensor_PPG_MAX30102’, 2020, [Online]. Available: https://github.com/Mic-Tsai/Sensor_ECG_PPG_MAX86150_Dev-Board

[73] P. van Gent, H. Farah, N. van Nes, and B. van Arem, ‘Analysing Noisy Driver Physiology Real-Time Using Off-the-Shelf Sensors: Heart Rate Analysis Software from the Taking the Fast Lane Project’, *Journal of Open Research Software*, Oct. 2019, doi: 10.5334/jors.241.

[74] P. van Gent, H. Farah, N. van Nes, and B. van Arem, ‘HeartPy: A novel heart rate algorithm for the analysis of noisy signals’, *Transportation Research Part F: Traffic Psychology and Behaviour*, vol. 66, pp. 368–378, 2019, doi: https://doi.org/10.1016/j.trf.2019.09.015.

[75] S. Ismail, U. Akram, and I. Siddiqi, ‘Heart rate tracking in photoplethysmography signals affected by motion artifacts: a review’, *EURASIP Journal on Advances in Signal Processing*, vol. 2021, no. 1, p. 5, Jan. 2021, doi: 10.1186/s13634-020-00714-2.

[76] Z. Zhang, Z. Pi, and B. Liu, ‘TROIKA: A General Framework for Heart Rate Monitoring Using Wrist-Type Photoplethysmographic Signals During Intensive Physical Exercise’, *IEEE Transactions on Biomedical Engineering*, vol. 62, no. 2, pp. 522–531, 2015, doi: 10.1109/TBME.2014.2359372.

[77] A. Temko, ‘Accurate Heart Rate Monitoring During Physical Exercises Using PPG’, *IEEE Transactions on Biomedical Engineering*, vol. 64, no. 9, pp. 2016–2024, 2017, doi: 10.1109/TBME.2017.2676243.

[78] W. Karlen, ‘CapnoBase IEEE TBME Respiratory Rate Benchmark’. [Online]. Available: https://doi.org/10.5683/SP2/NLB8IT

[79] W. Karlen, S. Raman, J. M. Ansermino, and G. A. Dumont, ‘Multiparameter Respiratory Rate Estimation From the Photoplethysmogram’, *IEEE Transactions on Biomedical Engineering*, vol. 60, no. 7, pp. 1946–1953, 2013, doi: 10.1109/TBME.2013.2246160.

[80] P. van Gent, ‘heartrate_analysis_Arduino’, 2019, [Online]. Available: https://github.com/paulvangentcom/heartrate_analysis_Arduino

Annex A

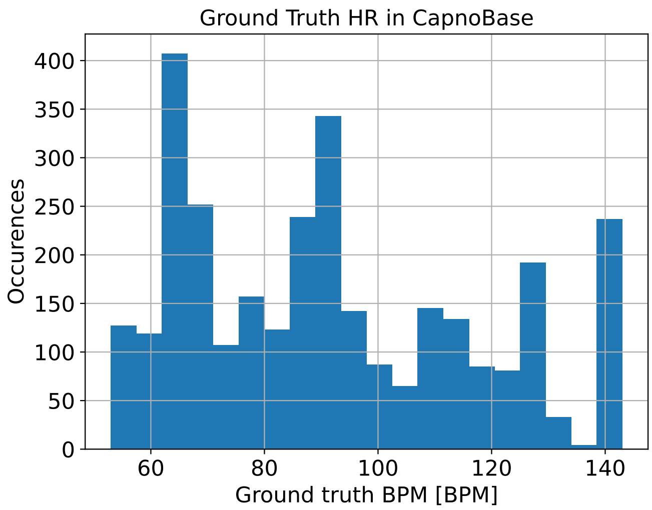

Figure 22: Distribution of ground truth HR values in the CapnoBase recordings with artefacts.

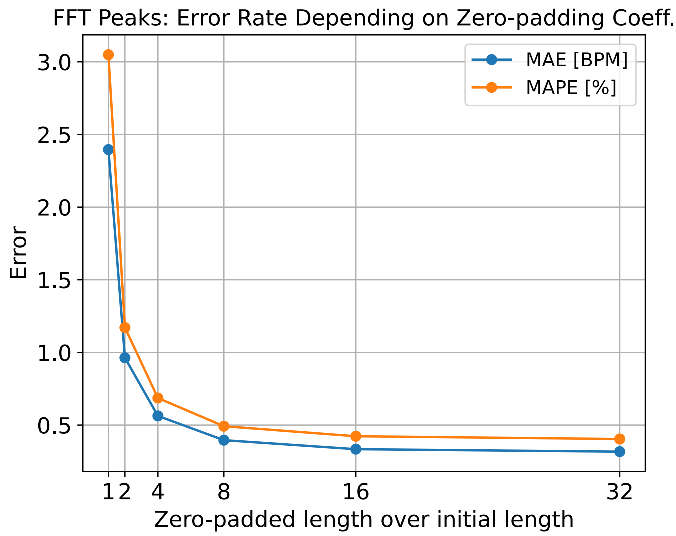

Figure 23: Influence of the zero-padding coefficient on the accuracy of the spectrum-based algorithm, evaluated using the CapnoBase dataset.

Category	Name	MAE [BPM]	MAPE [%]
Spectrum-based	FFT Peaks [68]	0.571	0.694
Peak-based	BIOBSS Beats [69]	1.660	1.739
Threshold-based	HeartPy [73], [74]	0.227	0.281
Dummy	Random (50–150 BPM)	29.672	36.088

Table 10: Accuracy of the best performers on the CapnoBase dataset with the PPG signal interpolated at 125 Hz.

UNIVERSITÉ CATHOLIQUE DE LOUVAIN
École polytechnique de Louvain
Rue Archimède, 1 bte L6.11.01, 1348 Louvain-la-Neuve, Belgique | **www.uclouvain.be/epl**